

# **Mutations in dihydrofolate reductase from *Escherichia coli*: Impact on aggregation, trimethoprim resistance and fitness**

A thesis

submitted to

Indian Institute of Science Education and Research, Pune

in partial fulfillment of the requirements for the

BS-MS Dual Degree Programme

by

**Swapnil Shankar Bodkhe**



Indian Institute of Science Education and Research Pune

Dr. Homi Bhabha Road

Pashan, Pune 411008, India

April 2018

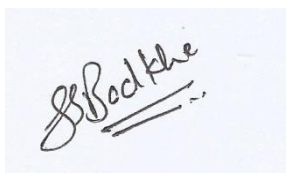
Supervisor: **Dr. Nishad Matange**

©Swapnil Bodkhe 2018

All rights reserved

# Certificate

This is to certify that this dissertation entitled "**Mutations in dihydrofolate reductase from Escherichia coli: Impact on aggregation, trimethoprim resistance and fitness**" towards the partial fulfillment of the BS-MS dual degree programme at the Indian Institute of Science Education and Research, Pune represents study/work carried out by **Swapnil Shankar Bodkhe**, at **IISER Pune** under the supervision of **Dr. Nishad Matange**, **DST-INSPIRE faculty fellow**, **Department of Biology, IISER Pune** during the academic year 2017-18.



**Swapnil Shankar Bodkhe,**  
**IISER Pune**




**Dr. Nishad Matange**  
**DST-INSPIRE Faculty Fellow,**  
**Department of Biology,**  
**IISER Pune**

**Date: 20<sup>th</sup> March 2018**

## Declaration

*I hereby declare that the matter embodied in the report entitled “Mutations in dihydrofolate reductase from Escherichia coli: Impact on aggregation, trimethoprim resistance and fitness” are the results of the work carried out by me at the Department of Biology at IISER Pune, under the supervision of Dr. Nishad Matange, DST-INSPIRE faculty fellow, Department of Biology, IISER Pune and the same has not been submitted elsewhere for any other degree.*



**Swapnil Shankar Bodkhe,**

**IISER Pune**



**Dr. Nishad Matange**

**DST-INSPIRE Faculty Fellow,**

**Department of Biology,**

**IISER Pune**

**Date: 20<sup>th</sup> March 2018**

# **Acknowledgments**

Foremost, I would like to express my gratitude towards Dr. Nishad Matange for giving me the opportunity to carry out the research work in his laboratory. The project would not have been successful without his constant guidance and support. His own enthusiasm towards the project and encouragement has really been driving force behind the project. I thank him for introducing to the field of microbiology and for mentoring not only in project work but also in outside matters. I would like to thank all my colleagues in our lab for wonderful discussions and insights into my project.

I thank our former and current Director Dr. K. N. Ganesh, Dr. Jayant Udgaonkar and chairperson of Biology department Dr. Sanjeev Galande for providing such a wonderful research atmosphere and facilities at IISER Pune. I thank my thesis advisor Dr. Girish Ratnaparkhi for his inputs in projects and helpful suggestions for the thesis. I would like to thank Dr. Nagraj Balasubramaniam and his lab members for helping me in carrying out some of the experiments in his laboratory. I also thank all the administrative staff, technical and non-technical staff for providing smooth service during project work.

I thank DST-INSPIRE and IISER Pune for the financial support to the research project.

I would like to thank my family and friends for their constant support to complete the project.

Swapnil Bodkhe

## **Table of Content**

<b>Content</b>	<b>Page no.</b>
<b>List of abbreviations</b>	<b>1</b>
<b>List of figures</b>	<b>2</b>
<b>List of tables</b>	<b>4</b>
<b>Abstract</b>	<b>5</b>
<b>Introduction</b>	<b>6</b>
<b>Materials and methods</b>	<b>16</b>
<b>Results and discussion</b>	<b>24</b>
<b>Summary and future directions</b>	<b>43</b>
<b>Appendix</b>	<b>46</b>
<b>Bibliography</b>	<b>48</b>

## List of Abbreviations

<b>Sign</b>	<b>Full form</b>	<b>Sign</b>	<b>Full form</b>
<b>°C</b>	Degree Celsius	<b>mg</b>	Milligram
<b>µg</b>	Microgram	<b>ng</b>	Nanogram
<b>G</b>	Gram	<b>kDa</b>	Kilo Dalton
<b>µM</b>	Micromolar	<b>nm</b>	Nanomolar
<b>mM</b>	Milimolar	<b>M</b>	Molar
<b>µL</b>	Microlitre	<b>mL</b>	Milliliter
<b>L</b>	Litre	<b>kb</b>	Kilo base pair
<b>bp</b>	Base pair	<b>OD</b>	Optical density
<b>rpm</b>	Revolution per minute	<b>PCR</b>	Polymerase chain reaction
<b>DHFR</b>	Dihydrofolate reductase	<b>mA</b>	Miliampere
<b>TMP</b>	Trimethoprim	<b>Ni-NTA</b>	Nickel-Nitrilotriacetic acid
<b>LB</b>	Luria Broth	<b>aa</b>	Amino acid
<b>dNTP</b>	Deoxyribonucleotide triphosphate	<b>IPTG</b>	Isopropyl-β-D-1-thyogalactopyranoside
<b>MIC</b>	Minimum inhibitory concentration	<b>IC50</b>	Inhibitory concentration for 50% growth
<b>SDS-PAGE</b>	Sodium dodecyl sulphate- Polyacrylamide gel electrophoresis	<b>EDTA</b>	Ethylenediaminetetraacetic acid

## List of Figures

<b>Figure no.</b>	<b>Legend</b>	<b>Page no.</b>
1.1	Schematic representation of various mechanisms of antibiotic resistance	7
1.2	DHFR crystal structure	13
1.3	Comparison of chemical structures of molecules	14
2.1	Western blot standardisation for endogenous expression of DHFR for different mutants	21
3.1	Solubility characterisation of wild type and mutant DHFR protein	24
3.2	DHFR crystal structure and Predictions of protein stability by iMutant2.0 software	25
3.3	Various interactions of residues in DHFR and their distances	27
3.4	Predictions of protein stability by iMutant2.0 software	28
3.5	Generation and screening of I155A on pPRO plasmid using site-directed mutagenesis	28
3.6	Solubility characterisation of wild type and mutant DHFR protein	29
3.7	Resistance level check for different strains using dilution assay	30
3.8	Dose response curve for strains having different mutations in DHFR	31
3.9	Probable interaction of residues after mutations	32

<b>Figure no.</b>	<b>Legend</b>	<b>Page no.</b>
3.10	Growth curves of different strains in LB medium	34
3.11	Growth curves of different strains in LB + thymidine (100 µg/mL) medium	34
3.12	Growth curves of different strains in LB + TMP (250 ng/mL) medium	35
3.13	Growth curves of different strains in M9 defined medium (with supplements)	35
3.14	Growth rates of TMP resistant strains in different medium	37
3.15	Comparison OD after 12 hours growth of TMP resistant strains in different medium	37
3.16	Fitness comparisons of TMP resistant strains in LB	38
3.17	Fitness comparisons of TMP resistant strains in LB	39
3.18	Western blot for endogenous expression of DHFR for different mutants in LB medium	41
3.19	Western blot for endogenous expression of DHFR for different mutants in M9 defined medium	42



## List of Tables

<b>Table no.</b>	<b>Legend</b>	<b>Page no.</b>
1.1	List of antibiotic and its target protein and representative organisms where the resistance was observed for the antibiotics	9
1.2	List of organisms where fitness cost was found for specific antibiotics in different assay system	11
2.1	Mutations generated on pPRO plasmid and the primers used for mutagenesis	18

## **Abstract**

Alteration of the structures of proteins due to non-synonymous substitutions can affect their biochemical functions either by perturbation of active sites geometry, decrease in expression level or aggregation and misfolding. These micro-level changes are translated to organism-level phenotypes like growth rate changes, which finally impact the fitness of an individual. The relationship between mutational changes and organism-level changes is referred to as the genotype-phenotype relationship. In this study, we are trying to establish the genotype-phenotype relationship for mutational changes in the metabolic enzyme dihydrofolate reductase (DHFR) in *Escherichia coli* that confer resistance to the antibiotic trimethoprim. DHFR is expressed as low-copy numbers whose activity is essential for purine and pyrimidine synthesis in bacteria. In this project it is demonstrated that a sub-set of trimethoprim-resistance associated mutations at W30 residue destabilise DHFR leading to its aggregation. Concurrently, some of these mutations are associated with lowered fitness relative to wild type. This decrease in fitness is most likely due to lowered expression and lowered activity of the mutant DHFR enzymes and not due to aggregation-associated cytotoxicity. Using this system, the ultimate aim is to delineate the relationship between expression level, solubility, stability and organismal fitness that would influence the selection dynamics of trimethoprim-resistant bacteria.

# **CHAPTER 1: INTRODUCTION**

## **1.1 Antibiotic resistance: a global threat**

Antibiotics or antimicrobial drugs are small-molecule chemicals which are either produced by microorganisms or made synthetically. They bind to specific target proteins interfering with their vital functions and result in killing or inhibiting the growth of bacteria (Waksman, 2011). Antibiotics are effective against bacterial infections but due to improper and rampant use, resistance against many of the available antibiotics is spreading all over the world making several infections untreatable (Laxminarayan et al., 2013). For instance, multidrug-resistant and extremely drug-resistant bacteria are started to emerge in case of tuberculosis (Böttger and Springer, 2008). Likewise, methicillin resistant *Staphylococcus aureus* (MRSA) is a common cause of community or hospital-associated infections. Resistance is now found to all  $\beta$ -lactams like ampicillin, methicillin making diseases like pneumonia and meningitis harder to treat (Otto, 2013).

Antibiotic resistance is thought to develop due to repeated use of antibiotics in treatment, allowing microbes to adapt to antibiotics in the environment. More recent research has found that even exposure to the low levels of antibiotics, far lower than inhibitory concentrations, can promote the evolution of resistance in bacteria. This situation is very dangerous as small levels of antibiotics are present in the environment due to pollution by pharmaceutical industries, hospitals and livestock which can lead to the spread of drug-resistant bacteria (Andersson and Hughes, 2014). To tackle this problem, there is a need to understand the different mechanisms and paths used by bacteria to resist antibiotics which will help in deciding the strategy to use the available antibiotics more effectively and also in the generation of new antibiotics.

## 1.2 Mechanisms of antibiotic resistance in bacteria:

Antibiotic resistance follows Darwinian evolution. In the presence of antibiotics, there is selection pressure on the bacteria which results in generation of resistant bacteria through random mutations. Eventually, resistant bacteria take over the population eliminating drug-sensitive bacteria altogether. Resistance causing mutations have been mapped to a number of different pathways (Figure 1.1). Following are some of the commonly encountered mechanisms of drug-resistance in clinically relevant bacterial infections:

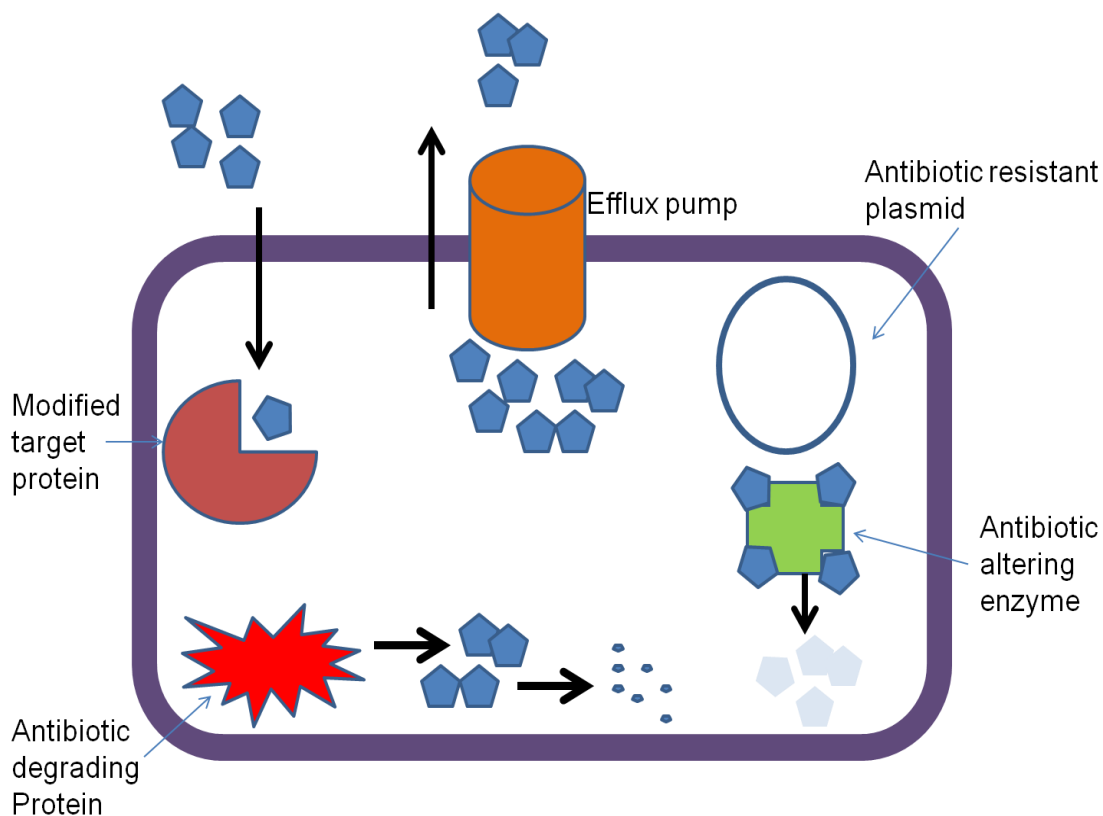


**Figure 1.1: Schematic representation of various mechanisms of antibiotic resistance**

### a) Activation of efflux pumps:

Bacterial innate efflux pumps usually remove small molecules from the cell (Nikaido, 1998). Some of these efflux pumps are able to remove the antibiotics out of the cell as well. Efflux pumps are widely present in gram-negative bacteria and gram-positive bacteria (Sun et al., 2014). Generally, these efflux pumps are not specific to any antibiotics and this leads to resistance to multiple drugs.

Resistance can be acquired by activation of efflux pumps in bacteria due to chromosomal mutations in the efflux pump genes. *AcrAB/TolC* is one of the examples of efflux pumps in *E. coli* (Riley et al., 2006). This system is generally dormant but it can be activated by mutation in *mdfA* gene which gives resistance against chloramphenicol and nalidixic acid (Baughman and Fahnestock, 1979). In *Neisseria gonorrhoea* due to overexpression of efflux pumps, resistance against azithromycin has been observed in the clinical setting (Zarantonelli et al., 2001).

b) Inactivation of antibiotics:

Bacteria can inactivate antibiotics by the generation of different drug inactivating enzymes. This system is commonly observed in beta-lactam resistant bacteria which have beta-lactamase proteins which degrade the antibiotics having beta-lactam ring such as penicillin, ampicillin, cefsulodin etc. (Bradford, 2001). Resistance to ampicillin, penicillin and cephalosporin in *E. coli* is commonly mediated by beta lactamases like TEM-1 which can hydrolyse the antibiotics. *Klebsiella pneumonia* is found to have resistance against ampicillin due to the presence of SHV-1 beta lactamase protein (Ghafourian et al., 2014). Some bacteria are also found to have aminoglycoside- inactivating enzymes which involve acetyltransferases, nucleotidyltransferase and phosphotransferase which give resistance against aminoglycosides such as streptomycin, spectinomycin and Gentamycin by enzyme inactivation. In *E. coli* resistance against apramycin is found due acetylation of the antibiotic by the enzyme. Similarly, due to adenylation and phosphorylation of antibiotics like spectinomycin and streptomycin, resistance has been observed in gram-negative bacteria as well as some gram-positive bacteria (Shaw et al., 1993).

c) Alteration of antibiotic target:

Another strategy of resistance uses alteration of the antibiotic target enzyme itself due to non-synonymous mutations in target protein gene. These mutations alter the structure of the target protein preventing antibiotic binding. This strategy of drug resistance is found against many antibiotics such as rifampicin, streptomycin, kanamycin, sulphamethoxazole, fusidic acid, novobiocin, nalidixic acid, ciprofloxacin, triclosan, trimethoprim, coumermycin etc (Andersson and

Hughes, 2010). Some of the cases of antibiotics for which resistance is developed due to target protein alteration are shown in table 1.1.

Antibiotic	Target	Resistance found in organism (representative)
Trimethoprim	Dihydrofolate reductase	<i>Escherichia coli</i>
Sulphamethaxazole	Dihydropteroate synthase	<i>Streptococcus pneumoniae</i>
Rifampicin	$\beta$ -subunit of RNA polymerase	<i>Mycobacterium tuberculosis</i>
Streptomycin	S-12 subunit of the ribosome	<i>Pseudomonas aeruginosa</i>
Triclosan	Enoyl-acyl carrier protein reductase	<i>Staphylococcus aureus</i>
Ciprofloxacin	DNA gyrase	<i>Acinetobacter haemolyticus</i>

**Table 1.1: List of antibiotic and its target protein and representative organisms where the resistance was observed**

d) Overexpression of target protein:

This process provides a low level of antibiotic resistance which is achieved by the mutations in the promoter region of target protein gene. Antibiotics bind to target proteins, but due to overexpression, bacteria have enough target protein to carry out the vital functions (Palmer and Kishony, 2014). This strategy was observed with few antibiotics such as trimethoprim, ampicillin, isoniazid and triclosan. Overexpression of target protein can have different effects on resistance and on the fitness of the bacteria. For example, overexpression of target protein in case of trimethoprim (Dihydrofolate reductase), coumermycin (DNA Gyrase) and triclosan (Enoyl-acyl carrier protein reductase) correlated with an increase in the resistance level but the resistance decreases in case of ciprofloxacin (DNA Gyrase) and cefsulodin (Penicillin binding protein 1A) due toxic activity of enzyme and substrate.

### **1.3 Horizontal acquisition of antibiotic resistance:**

Antibiotic resistance spreads horizontally along with vertical transmission with the help of plasmids. Antibiotic resistance genes are transferred to susceptible bacteria in the population via plasmids and can lead to the rapid spread of resistance in the population (Ramirez et al., 2014). Gram-negative bacteria such as *Klebsiella pneumonia* have been found to have plasmids which confer resistance to antibiotics such as cephalosporins, carbapenems, aminoglycosides and fluoroquinolones. Resistance to  $\beta$ -lactam antibiotics is also spread through the transfer of a  $\beta$ -lactamase gene from plasmids in gram-negative bacteria (Saunders et al., 1986). Phages can also transfer the antibiotic resistance genes horizontally. New evidence suggests that phages may act as reservoirs of antibiotic resistance genes. Beta-lactamase genes which can give resistance to last resort antibiotics are carried by phages which have different host range. Phages like siphoviridae, podoviridae and myoviridae carry antibiotic resistance genes and transfect bacteria like actinobacteria, alpha-proteobacteria and beta-proteobacteria (Subirats et al., 2016).

This project deals with mutations that lead to non-synonymous substitutions in proteins. These mutations are commonly encountered in drug resistant bacteria. It was realized that in addition to conferring drug resistance, such substitutions may also alter other properties of the protein, such as its ability to fold properly or its enzymatic efficiency. Such changes can affect the fitness of drug-resistant bacteria and hence govern the selection dynamics of antibiotic resistance. A few examples of these are discussed in the following section.

### **1.4 Effects of antibiotic resistance conferring mutations on target proteins:**

Proteins are marginally stable, meaning that only specific structures are allowed in order to minimize the Gibbs free energy (Klesmith et al., 2017). Mutations can change the amino acid sequences and hence the structure of proteins. These changes can have beneficial, neutral or deleterious effects on stability and function of proteins (Studer et al., 2013). Proteins follow the law of natural selection and evolve under it. Generally speaking, mutations which increase the stability of a protein tend to decrease the catalytic activity. Also, mutations at the active site and the buried residues are less prone to mutations than the residues at binding cavity and residues at the periphery of protein (Klesmith et al., 2017; Studer et al., 2013). In

antibiotic resistance, there is a change in the amino acids sequence of target protein at specific sites. As different proteins have different tolerance to the mutations, the effects drug resistance conferring mutations on proteins and on fitness will be different in case of various antibiotics. As a result, resistance phenotypes are often associated with fitness costs in the absence of antibiotics. Table 1.2 shows the presence of cost in different bacteria for different antibiotic resistance.

Organism	Antibiotic	Assay system	Fitness cost
<i>Salmonella enterica subspecies enterica serovar Typhimurium</i>	Streptomycin	Mice and in vitro	Variable
	Rifampicin	Mice and in vitro	Variable
	Nalidixic acid	Mice and in vitro	Yes
	Ciprofloxacin	Chicken and in vitro	Yes
	Fusidic acid	Mice and in vitro	Variable
<i>Escherichia coli</i>	Streptomycin	in vitro	Variable
	Norfloxacin	Mice and in vitro	Variable
	Rifampicin	in vitro	Variable
	Fosomycin	Urine and in vitro	Yes
	Trimethoprim	In vitro	Variable
<i>Staphylococcus aureus</i>	Fusidic acid	Rats and in vitro	Variable
	Rifampicin	Biofilm and in vitro	Variable
	Mupiricin	Mice and in vitro	No
	Methicillin	in vitro	Yes
	Vancomycin	in vitro	Variable

**Table 1.2: List of some representative bacteria where fitness cost was found due to antibiotic resistance conferring mutations in case of antibiotics in different assay system {Adapted from (Andersson and Hughes, 2010)}.**

Fitness cost associated with antibiotic resistance is variable and also dependent upon the environment in which fitness is assessed. Further, the magnitude of fitness cost for resistance to an antibiotic depends on the mutations and its position. Generally, fitness costs of drug resistance depend on the nature of enzymatic processes which are affected by resistance-conferring mutations. For instance, antibiotic resistance-conferring mutations which affect processes like translation and

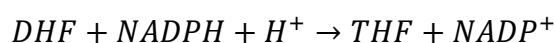


transcription, decreases the efficiency of these processes leading to slower cell will divide and a fitness cost (Vogwill and Maclean, 2015). This is not observed in the case of non-target protein like beta lactamases as beta lactamase is not involved in the production of vital metabolites. Lack of fitness cost has resulted in the evolution of thousands of beta lactamases variants which are called extended spectrum of beta lactamases (ESBL) (Jacquier et al., 2013). Thus, mutations in target protein which is involved in the vital metabolic process are more likely to be costly.

### 1.5 Trimethoprim and DHFR:

Trimethoprim is a wide spectrum antibiotic which binds to dihydrofolate reductase (DHFR) and inhibits it, preventing the growth of some gram-negative as well as gram-positive bacteria. It is widely used against urinary tract infections, pneumonia, otitis media along with sulphamethoxazole (Watson et al., 2007). Resistance against trimethoprim in *Streptococcus pneumoniae* was first found in 1972 and is now found in various different pathogens (Maskell et al., 2001).

DHFR is a small monomeric protein around ~18 kDa (159 aa) which catalyses the conversion of dihydrofolate (DHF) to tetrahydrofolate (THF) which is a vital step in the biosynthesis of glycine, methionine, purines and thymidine.



DHFR is present in low amount in *E. coli* (approximately 40 copies/cell) and is essential for growth (Watson et al., 2007). However, *E. coli* can survive without DHFR if thymidine is provided exogenously in the growth medium.

Crystal structure of DHFR (Figure 1.2) from *E. coli* has been solved (PDB ID: 7DFR) (Bystroff et al., 1990). *E. coli* DHFR has eight beta sheets (designated as A-H) and four alpha helices ( $\alpha$ B,  $\alpha$ C,  $\alpha$ E and  $\alpha$ F). It has a binding domain for NADPH from residue 38 to 88 and three different loops namely Met 20 loop (9-24), F-G (116-132), G-H (142-150). The binding of substrates is ordered. First NADPH binds to the DHFR enzyme, followed by DHF. This results in the release of NADP<sup>+</sup> followed by binding of another molecule of NADPH and subsequent release of THF. The Met 20 loop is important for catalysis (Figure 1.2) as it changes the active site conformation through its motion (Boehr et al., 2006). The conformation of the Met-20 loop is

'closed' in the absence of DHF and NADPH binding. Upon formation of THF and NADP<sup>+</sup> forms, the conformation changes to 'occluded' state where it sterically hinders the binding of nicotinamide to the active site. The closed conformation brings the substrate and cofactor in close proximity within active site pocket (Schnell et al., 2004).

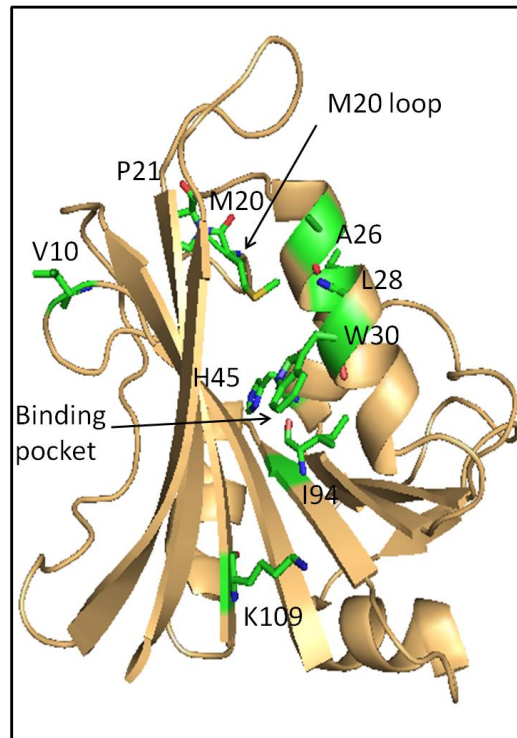


**Figure 1.2: DHFR crystal structure:** *E. coli* DHFR crystal structure (PDB id: 7DFR and resolution 2.5 Å) with residues which are mutated in trimethoprim resistant strains shown as sticks. M20 loop and the binding pocket for DHF are also shown. The image was generated using PyMOL software.

Trimethoprim is a competitive inhibitor of DHFR and competes with DHF (Figure 1.3 A, B and C), halting the reaction of THF formation. Methotrexate (Figure 1.3 D) is another competitive inhibitor of DHFR which is used as a chemotherapeutic agent in cancer. Trimethoprim has a higher affinity for *E. coli* DHFR than human DHFR while methotrexate binds human DHFR far better than bacterial DHFRs. Human and *E. coli* DHFR are structurally similar but differ in primary sequence and have different kinetics and different rate limiting steps (Bhabha et al., 2013). Bacteria have been reported to develop resistance against trimethoprim in three different ways:

overexpression of DHFR by mutations in promoter region of *folA* gene, alteration of DHFR sequence by mutations in *folA* structural gene (which codes for DHFR protein) and overexpression of structurally altered DHFR by both mutations in promoter region and in coding region of *folA* (Flensburg and Sköld, 1987; Palmer et al., 2015). Trimethoprim resistance can also occur due to the presence of plasmid which carries the *dhfr* genes (which codes for mutated DHFR). Till now 30 *dhfr* genes are found and these are associated with integrons, spread horizontally and spread trimethoprim resistance (Brolund et al., 2010). Trimethoprim and DHFR are ideal to study the effects of mutations on enzyme activity and functionality as most of the resistance-conferring mutations mapped in *folA* gene and promoter region which codes for DHFR. It is also a monomeric protein making it ideal to study genotype and phenotype linkage study.

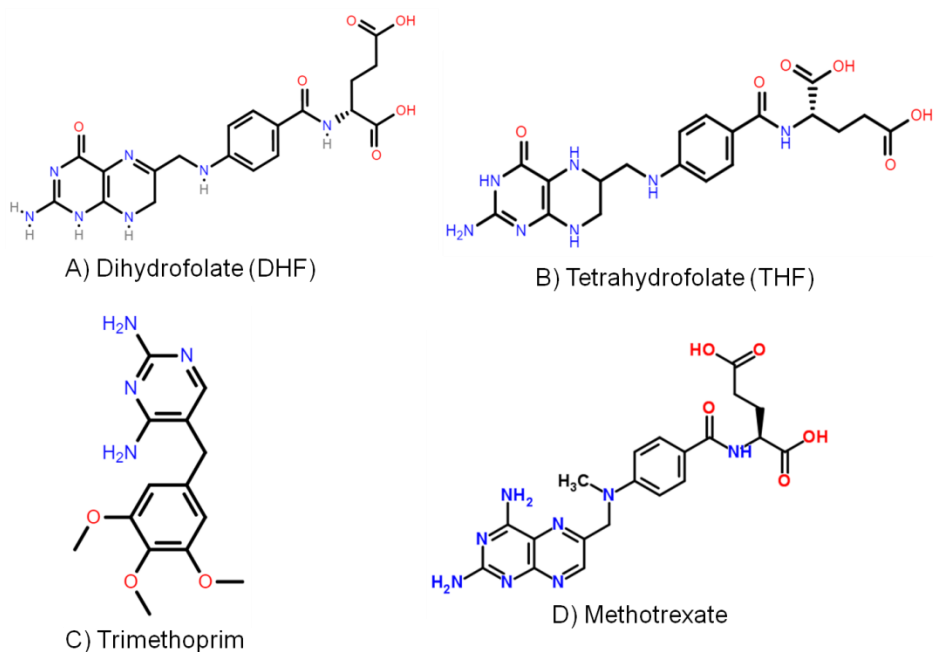


**Figure 1.3: Comparison of chemical structures of molecules:** A) Structure of dihydrofolate (DHF) which is the substrate for DHFR B) Structure of tetrahydrofolate (THF) which is released as product after catalysis by DHFR C) Trimethoprim structure which is inhibitor of *E. coli* DHFR D) Methotrexate structure which is an inhibitor of human DHFR.

## 1.6 Aim:

The main goal of the present study is to investigate the effects of trimethoprim resistance-conferring mutations on DHFR at the molecular level and at phenotypic level in *E. coli*. In preliminary experiments, using site-directed mutagenesis on a plasmid-encoded copy of wild type DHFR, mutations which are known to confer trimethoprim resistance were engineered and the solubility of wild type and mutant DHFR enzymes was compared to infer the impact that TMP-resistant mutations have on the ability of DHFR to fold correctly. It was found that TMP-resistant mutations at the W30 position are largely insoluble and based on this it was hypothesized that these mutations promote aggregation/misfolding of DHFR. Trimethoprim-resistant strains were also selected under constant sublethal doses of trimethoprim and W30G, W30C, P21Q and P21L mutations on the chromosome were obtained. In this project, the goal was to find a structural explanation for why W30 mutations cause aggregation of DHFR and to investigate the fitness cost associated with TMP-resistance in *E. coli*. Understanding the relation between the expression level of DHFR, trimethoprim resistance and fitness in *E. coli* from studies like this one will help in elucidating the selection dynamics of antibiotic-resistant bacteria.

# **CHAPTER 2: MATERIALS AND METHODS**

## **2.1: Strains, culture conditions and materials:**

*E. coli* K-12 MG1655 strain (Genotype: F<sup>-</sup>, lambda<sup>-</sup>, rph-1) was used as the wild type for most of the experiments and *E. coli* NEB Turbo cells were used for DNA manipulation. Both strains were available in the laboratory. Luria-Bertani broth (LB) (HiMedia, India) was used for routine cultures and LB-Agar (LA) (HiMedia, India) was used for streaking and plating purposes. For defined media experiments, M9 defined medium (HiMedia, India) with glucose (0.2%), casein hydrolysate (0.1%) and thiamine (0.5 µg/mL) was used. All cultures were grown at 37° C and at 180 rpm shaking. The pPRO-HTb and pBKS plasmids as well as pPRO-HTb-foIA and pBKS-foIA plasmids were available in the laboratory and used for cloning and mutagenesis purposes. Fine chemicals were purchased from MP Biomedicals, India and Sigma Lifesciences, U.S. Restriction enzymes were purchased from New England Biolabs, U.K. Solvents used in this project were from Fischer Scientific U.S.A and were available in the common stock of IISER Pune. Anti-DHFR polyclonal antibody was available in the laboratory.

## **2.2: Preparation of chemically competent cells:**

A single colony of *E. coli* was inoculated into LB broth (2 mL) and incubated overnight at 37°C with shaking at 180 rpm (Innova 42 & 42 R incubator, New Brunswick Scientific). The overnight grown cultures were passaged (1%) into LB broth (100 mL) and grown for 2 hours at 37°C with shaking at 180 rpm. Cultures were cooled for 30 minutes on ice and harvested by centrifugation at 3000 rpm for 10 minutes (5810 R Eppendorf, Germany). The bacterial pellets were washed twice with 10 mL sterile CaCl<sub>2</sub> (0.1 M) and incubated on ice for 20 minutes. Resuspended cells were harvested by centrifugation at 4000Xg for 5-10 minutes. The pellets were finally resuspended in sterile CaCl<sub>2</sub> (0.1 M) + glycerol (15%) and aliquoted (100 µL) in 1.5 mL sterile tubes and stored at -80°C until further use.

## **2.3: Transformation of plasmid DNA:**

Competent cells were thawed on ice and plasmid DNA (0.5 µL) was added. The tubes were mixed gently by tapping and incubated for 10-15 minutes on ice. The

tubes were then transferred to 37°C on a thermomixer (Eppendorf ThermoMixer C, Germany) for 2 minutes and immediately transferred back to the ice. Sterile LB broth (1 mL) was added and incubated at 37°C with shaking at 180 rpm. Bacterial cells were harvested by centrifugation, spread on a plate containing media supplemented with the appropriate antibiotic and incubated for 12-15 hours at 37°C.

#### **2.4: Plasmid Isolation:**

Bacterial cultures were grown in LB broth (3 mL) overnight. Overnight grown cultures were harvested by centrifugation at 12000 rpm for 30 seconds (5430 R, Eppendorf, Germany). The pellet was resuspended in 200 µL Solution I (50 mM glucose, 25 mM Tris-HCl pH 7.5, 10 mM EDTA) by vortexing. Lysis was carried out by the addition of 200 µL of Solution II (0.2 N NaOH, 1% SDS) and incubation for 1-2 minutes at room temperature. The solution was neutralized with 200 µL of Solution III (5 M Potassium acetate, 2.01M acetic acid). Finally, the solution was extracted with 300 µL of chloroform. Aqueous and organic phases were separated by centrifugation at 12000 rpm for 3 minutes (5430 R, Eppendorf, Germany). The aqueous layer was transferred to a fresh tube and isopropyl alcohol (650 µL) was added to precipitate the plasmid DNA. The tubes were centrifuged at 12000 rpm for 5-7 minutes and the pellets were washed with 500 µL chilled 70% ethanol. The pellets were dried and resuspended in 30 µL Tris-EDTA buffer supplemented with RNase (100 µg/mL).

#### **2.5: Site-directed mutagenesis and sub-cloning:**

Mutations were created in dihydrofolate reductase gene (*folA*) using site-directed mutagenesis. The protocol was adapted from published literature (Shenoy and Visweswariah, 2003). The pPRO-HTb-*folA* plasmid (available in the laboratory) (which has a (His)<sub>6</sub>-tag, a hybrid *Lac* promoter, multiple cloning site with ampicillin marker) was used as a template for generation of F137A and F153A mutations. pBKS-*folA* (has multiple cloning site with ampicillin marker and no promoter) was used for generation of I155A mutation (Vector maps of pBKS and pPRO are shown in appendix). For each mutation, different mutagenic primers were designed using the Sitefind tool ([www.bioinformatics.org/sitefind/SiteFind.html](http://www.bioinformatics.org/sitefind/SiteFind.html)). Using these primers (Table 2.1), whole plasmid polymerase chain reaction (PCR) was done and *DpnI*

enzyme was added to digest the methylated template plasmid. The mutated plasmids were transformed into *E. coli* NEB turbo cells and mutants were selected on ampicillin plates (100 µg/mL). The isolated plasmids were screened using specific restriction enzymes and clones were sent for the confirmation of mutants by sequencing. Sequencing services were provided by First Base sequencing, Malaysia. Mutations that were created in pBKS plasmid were sub-cloned in pPRO-HTb. For subcloning, *folA* gene was released from pBKS-*folA* using *EcoRV*, *NotI* digestion and pPRO-HTb was cut with *StuI*, *NotI* digestion overnight at 37°C. Cut *folA* gene and pPRO plasmid were purified using GeneClean kit II (MP Biomedicals) and ligated using T4 DNA ligase at room temperature for 1 hour. Ligated products were transformed into *E. coli* NEB turbo cells and selected on ampicillin plates (100 µg/mL). Isolated plasmids were screened using *PvuI*. For further experiments, mutated plasmids were transformed into *E. coli* MG1655 cells.

Mutation	Primer used
I155A	5'CAGCTATTGCTTTGAGGCTCTGGAGCGGCGGGGCC3'
I155T	5'CAGCTATTGCTTTGAGACTCTGGAGCGGCGGGGCC3'
I155D	5'CAGCTATTGCTTTGAGGATCTGGAGCGGCGGGG3'
F137A	5'ATGACTGGGAATCGGTAGCCAGCGAATTCCACGAT3'
F153A	5'CTCTCACAGCTATTGCGCTGAGATTCTGGAGCGG3'

**Table 2.1: Mutations generated on the pPRO plasmid and the primers used for mutagenesis**

## **2.6: Solubility characterisation of DHFR and its mutants:**

*E. coli* expressing the various mutant DHFR enzymes were inoculated in LB (1 mL) from frozen stocks and grown overnight at 37°C. Overnight grown cultures were further sub-cultured (1 %) into fresh LB (10 mL) for 2 hours and then DHFR proteins were induced with IPTG (500 µM) for 3 hours at 37°C or 15 hours at 18° C. Cultures were centrifuged at 4000 rpm for 5 minutes at 4°C. Pellets were resuspended in 1 mL of lysis buffer (50 mM Tris-HCl, 100 mM NaCl, 5 mM beta-mercaptoethanol and 10% glycerol). The suspensions were lysed using sonication (Time: 2 minutes 30 seconds, pulse: 10 sec off, 10 sec on, amplitude: 60%) (Sonics and materials,

U.S.A.). The lysates were first centrifuged at 1000 rcf for removal of un-lysed cells and then at 20000 rcf at 4°C to separate soluble and insoluble fractions. Pellets were resuspended in an equivalent amount of lysis buffer. SDS-PAGE was performed for equivalent amounts of lysates, pellets, and supernatants and the gels were stained with Coomassie Brilliant Blue R-250 for visualisation.

### **2.7: Isolation of trimethoprim-resistant mutant *E. coli*:**

Trimethoprim sensitive, wild-type *E. coli* populations were selected under daily exposure of 250 ng/mL trimethoprim for 8 days in a 96-well plate. Each day 10 % of the culture was subcultured. For control populations, trimethoprim was not added. The plate was incubated each day at 37°C with shaking at 150 rpm. Four trimethoprim-resistant populations were obtained after 8 days of selection. These were plated on 1 µg/mL trimethoprim plates to select drug-resistant isolates. Resistant colonies were isolated and characterized. For confirmation of mutants, *folA* locus was amplified from genomic DNA using forward primer *folA*<sub>prom\_XbaI\_fwd</sub> (5'CGGATTCTAGAGAAACGAAACCCTCATCC3') and reverse primer *folA*<sub>HindIII\_rev</sub> (5'GGCGAAGCTTCGGCGTCTTAAACACAGCC3') and sequenced.

### **2.8: Resistance level check:**

Strains were grown overnight in LB (1 mL) from frozen stocks. The cultures were diluted ten-fold serially in sterile 1X M9 medium (without supplements) and from each dilution 5 µL were spotted on 0, 1, 2, 4, 8 µg/mL TMP containing plates. The maximum dilution up to which bacterial growth was observed after 20-24 hours at 37 °C was noted down and the graph of maximum dilution and concentration of antibiotic was plotted.

### **2.9: Affinity purification of anti-DHFR antibody:**

The protocol was adapted from Chumpia et al. 2003 (Chumpia et al., 2003). Anti-DHFR serum (3 mL) was pre-cleared by incubation with 500µL Ni-NTA beads (BIO-RAD Laboratories) in the presence of triton-X 100 (0.1%) followed by centrifugation (2000rpm, 4°C, 1min). His-tagged DHFR protein was purified from *E. coli* harboring the pPRO-*folA* plasmid and incubated with 100µL Ni beads for binding (1 hour, 4°C). Unbound protein was cleared by centrifugation (30 sec, 3000 rpm). DHFR-bound



beads were incubated with pre-cleared serum for 12 hours at 4°C to allow binding of the anti-DHFR antibody to the beads. Beads were washed with 20 mL of DHFR-lysis buffer (50 mM Tris-HCl, 100 mM NaCl, and 10% glycerol). The antibody was eluted with different elution buffers (20 mM Tris-HCl, 0.15 M NaCl containing 1 M, 2 M, 4 M or 6 M guanidine hydrochloride) and the absorbance at 280 nm was measured. The eluate with the highest concentration of protein was subjected to desalting to eliminate imidazole. The desalted antibody was used for Western blot analysis.

### **2.10: Standardisation of Western blot analysis to establish a relation between expression of DHFR and fitness cost:**

Initially, expression levels were checked of DHFR and its mutants W30G, W30C and P21Q relative to wild-type DHFR using the anti-DHFR serum (1:5000) and the  $\Delta foIA$  strain was used as negative control (Figure 2.1). However, a lot of nonspecific binding was found which made the blot difficult to analyse (Figure 2.1 A). In an attempt to reduce the non-specific binding, lysates were centrifuged and only soluble fractions were subjected to Western blot. This did not significantly reduce non-specific binding (Figure 2.1B). Hence, standardisation of the Western on wild-type and  $\Delta foIA$  strains was undertaken. Further, it was thought that anti-DHFR serum had some affinity to other proteins also. For this problem, purification of anti-DHFR was done using affinity-based purification (Material and methods). Using affinity purified anti-DHFR IgG did not significantly reduce non-specific immunoreactivity (Figure 2.1 C). The amount of lysate protein in all these experiments was 10µg. To further standardise the process, different amount of proteins and total (anti-DHFR) IgG were used instead of serum as an antibody (Figure 2.1 D, E). There was a reduction in non-specific binding as seen in Figure 3.17 D and E. The little signal in  $\Delta foIA$  strains might be coming from nonspecific binding. From these experiments, amounts of lysate protein (5 µg) and concentration of antibody (100 ng/mL) were standardised.

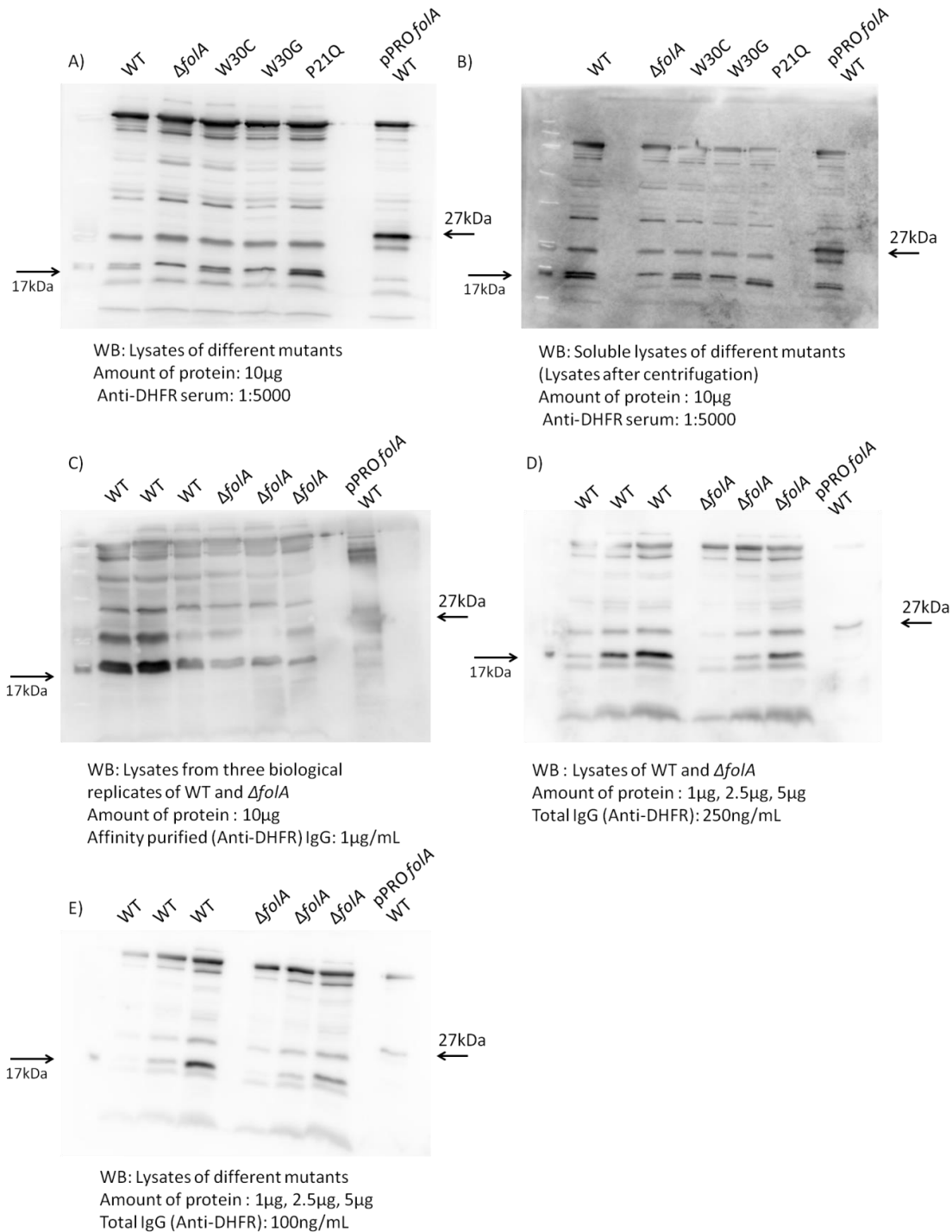


**Figure 2.1: Western blot standardisation for natural expression of DHFR.** Lysates of WT and DHFR mutants with different amounts were loaded and various concentrations of antibodies (anti-DHFR) were used for immunoblotting. Details of each blot are given: A) Lysates of DHFR mutants along with wild-type and  $\Delta folA$  strain (10 $\mu$ g). Anti-DHFR serum (1:5000) used as antibody. Lysate of pPROfolAWT is a positive control B) Soluble fractions of lysates of different DHFR mutants (10 $\mu$ g). Anti-DHFR serum (1:5000) used as antibody C) Lysates of wild-type and  $\Delta folA$  strain (10 $\mu$ g). Purified anti-DHFR serum eluted with 4M Gn-HCl (1  $\mu$ g/mL) used as antibody C) Lysates of wild-type and

*ΔfolA strain* (10μg). Purified anti-DHFR serum eluted with 4M Gn-HCl (1 μg/mL) used as antibody D) Lysates of wild-type and *ΔfolA strain* (1μg, 2.5 μg, 5 μg respectively) with 250 ng/mL anti-DHFR IgG E) Lysates of wild-type and *ΔfolA strain* (1μg, 2.5 μg, 5 μg respectively) with 100 ng/mL anti-DHFR IgG.

### **2.11: Checking expression level of endogenous DHFR:**

Test strains were grown overnight and then 1 % was sub-cultured in fresh LB for 3 hours. Cultures were centrifuged and resuspended in lysis buffer. Lysates were prepared by sonication (Time: 2 minutes 30 seconds, pulse: 10 sec off, 10 sec on, amplitude: 60%) (Sonics and materials, U.S.A.). The protein concentrations in lysates were measured by Bradford assay (Bradford, 1976). For an equal amount of total lysate protein (5μg), SDS-PAGE was performed and electrophoresed proteins were transferred to PVDF membrane (Merck Life Sciences, India) (size: 0.45 μm) by applying a constant current of 200 mA for 2 hours. The membrane was blocked with 5 % skimmed milk for 1 hour at room temperature. The membrane was probed with the anti-DHFR serum or purified anti-DHFR serum or total IgG (100 ng/mL) along with 0.5% BSA (SRL chemicals, India) in Tris-buffer saline-tween 20 (TBST: 10 mM Tris-HCl, 0.9% NaCl and 0.1% tween 20) overnight at 4°C. The membrane was then washed with TBST 3 times for 10 minutes each followed by incubation for 1 hour in secondary HRP-linked anti-rabbit antibody (Thermo Scientific) at room temperature. Excess of antibody was washed with TBST 3 times for 10 minutes each. Bound antibody was detected by chemiluminescence (Immobilon Western Chemiluminescent HRP substrate).

### **2.12: Competitive fitness assay:**

Test and reference strain (*ΔlacZ*) grown overnight in LB were mixed 1:1 in media (LB or defined media) at a starting density of  $\sim 10^6$  cells/mL. These strains were allowed to compete for 12 hours at 37°C (180 rpm shaking). The mixture was serially diluted and plated on LA plates containing X-Gal (40 μg/mL) and IPTG (1000 μM) after 0 and 12 hours of competition. Blue and white colonies were counted and relative fitness calculated according to following equation (Wiser and Lenski, 2015):

$$w = \ln(B_f / B_i) / \ln(A_f / A_i)$$

where  $A_f$ ,  $A_i$ , and  $B_f$ ,  $B_i$  are final and initial populations of two different strains.

### **2.13: Growth rate assay:**

Mutant or wild-type *E. coli* strains were grown overnight from frozen stocks in LB (1 mL) and 1% of the culture was transferred into fresh medium (LB or defined media) in 96 well plates. Each well had a final volume of 150  $\mu$ L. For each growth condition, three technical replicates were set up. Optical density (OD) at 600 nm was measured at 10 minutes intervals for 12 hours using a plate reader (Varioskan, Thermo Scientific). The plate was incubated at 37°C with 600 rpm orbital shaking. Maximum ODs were recorded to represent carrying capacities of strains. Growth rates were measured by obtaining the maximum rate of  $\Delta \ln$  OD vs time.

# CHAPTER 3: RESULTS AND DISCUSSION

## 3.1: Solubility characterisation of trimethoprim mutations:

To check the effects of trimethoprim resistance conferring mutations on the solubility of dihydrofolate reductase (DHFR) in *Escherichia coli* (*E. coli*), solubility characterisation were done previously on some mutations in *folA* gene (Figure 3.1). Point mutations known to confer trimethoprim-resistance were introduced into a plasmid borne-copy of the *folA* gene using site-directed mutagenesis. These mutations were distributed all over the DHFR protein as shown in Figure 3.2 A. Most of the overexpressed DHFR mutants were localized to the soluble fraction like the wild-type protein, as shown in Figure 3.1. However, mutant DHFR proteins with non-synonymous substitution at the 30<sup>th</sup> position, i.e. W30G, W30C and W30R were found primarily in the pellet fraction showing that these mutant DHFRs were prone to aggregation. The P21Q mutation was equally distributed between the pellet and supernatant fraction.

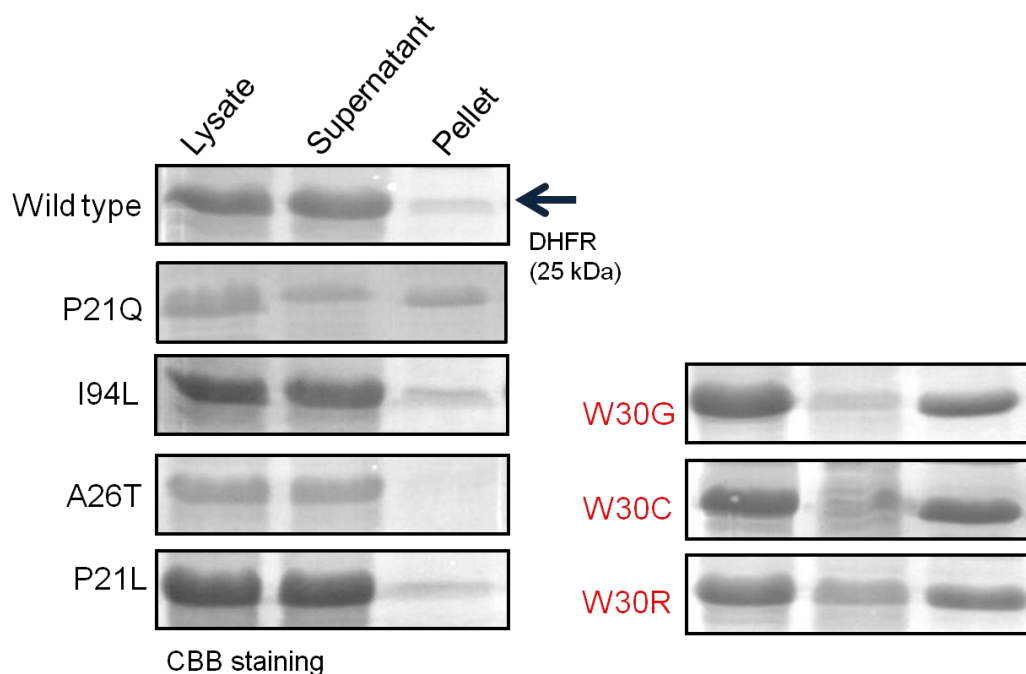


**Figure 3.1: Solubility characterisation of overexpressed wild type and mutant DHFR proteins:** Lysate, supernatant and pellet fractions of wild type DHFR and different mutant DHFRs subjected to SDS PAGE and visualized by staining with Coomassie.

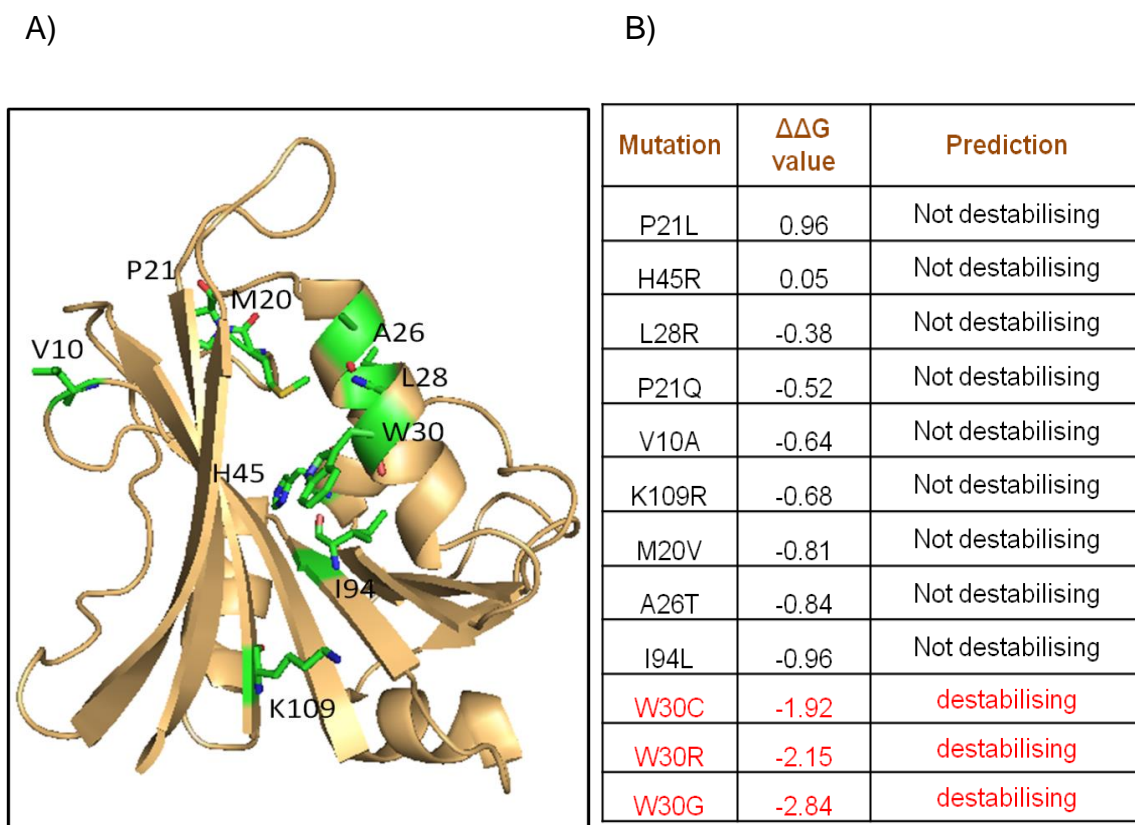


**Figure 3.2: DHFR crystal structure and Predictions of protein stability by iMutant2.0 software:** **A)** Trimethoprim resistance prone residues are shown on DHFR crystal structure. **B)** Stability predictions of DHFR by iMutant 2.0 are shown for different trimethoprim resistance conferring mutations. The table shows the difference of Gibb's free energy between wild-type protein and mutated protein ( $\Delta\Delta G = \Delta G_{\text{wild-type}} - \Delta G_{\text{mutant}}$ ) ( $\Delta\Delta G < 0$ : destabilising,  $\Delta\Delta G > 0$ : not destabilising)

The reason for the difference in solubility for different DHFR mutant may lie in the nature of the substitution. In case of P21L and I94L, a nonpolar residue is replaced with another nonpolar residue which probably does not have a large effect on structure; therefore, P21L and I94L DHFR are soluble. In case of P21Q, proline which is nonpolar is replaced by glutamine which is a polar residue and also has a longer side-chain than proline. This may affect the structure of DHFR more dramatically and consequently reduce the solubility of P21Q DHFR. In A26T, a nonpolar residue is replaced with polar as the P21 residue lies on the loop the structural perturbation will be less, so this might be the reason behind solubility of A26T. But in the case of W30G, W30C and W30R where tryptophan which is a

hydrophobic residue which is a part of alpha helix and present in a buried part of the protein is changed to hydrophilic amino acid (R and C) or an amino acid with different length (G) which might result into the creation of a cavity causing destabilisation of the structure. Since all the tested mutations at W30 in DHFR were prone to aggregation it was concluded that the stability and solubility of DHFR were dependent on the presence of W at the 30<sup>th</sup> position.

### **3.2: Structural and computational analysis of the impact of TMP resistant mutations on the stability of DHFR:**

Using computational tools, predictions about the effects of single site mutations on the stability of a protein can be made. iMutant 2.0 (Capriotti et al., 2005) is one such tool which can predict the stability effects of single site mutations using the crystal structure of the wild type protein as a reference and mutated residue as input. It measures the difference between  $\Delta G$  of folding of the mutant protein and wild type (i.e.  $\Delta\Delta G$ ). If the  $\Delta\Delta G$  value is between 0 and -1, then the mutation is predicted to be slightly destabilising and for values  $< -1$ , the prediction is a highly destabilising mutation. iMutant 2.0 was used to predict the effects of trimethoprim resistance mutations on the stability of DHFR. The iMutant results predicted that the W30G, W30R and W30G mutations were destabilising compared to other residue positions, corroborating the results described in Section 3.1 (Figure 3.2 B).

To understand why mutations at W30 altered the stability of DHFR, the crystal structure of *E. coli* DHFR (PDB ID: 7DFR) was analysed (Bystroff et al., 1990). W30 is present on an alpha helix that forms part of the binding site for dihydrofolate (DHF). Interestingly, the F137, F153 and I155 residues were all present within 4 Å distance of the side chain of W30 (Figure 3.3) indicating a possible hydrophobic interaction between them and W30.

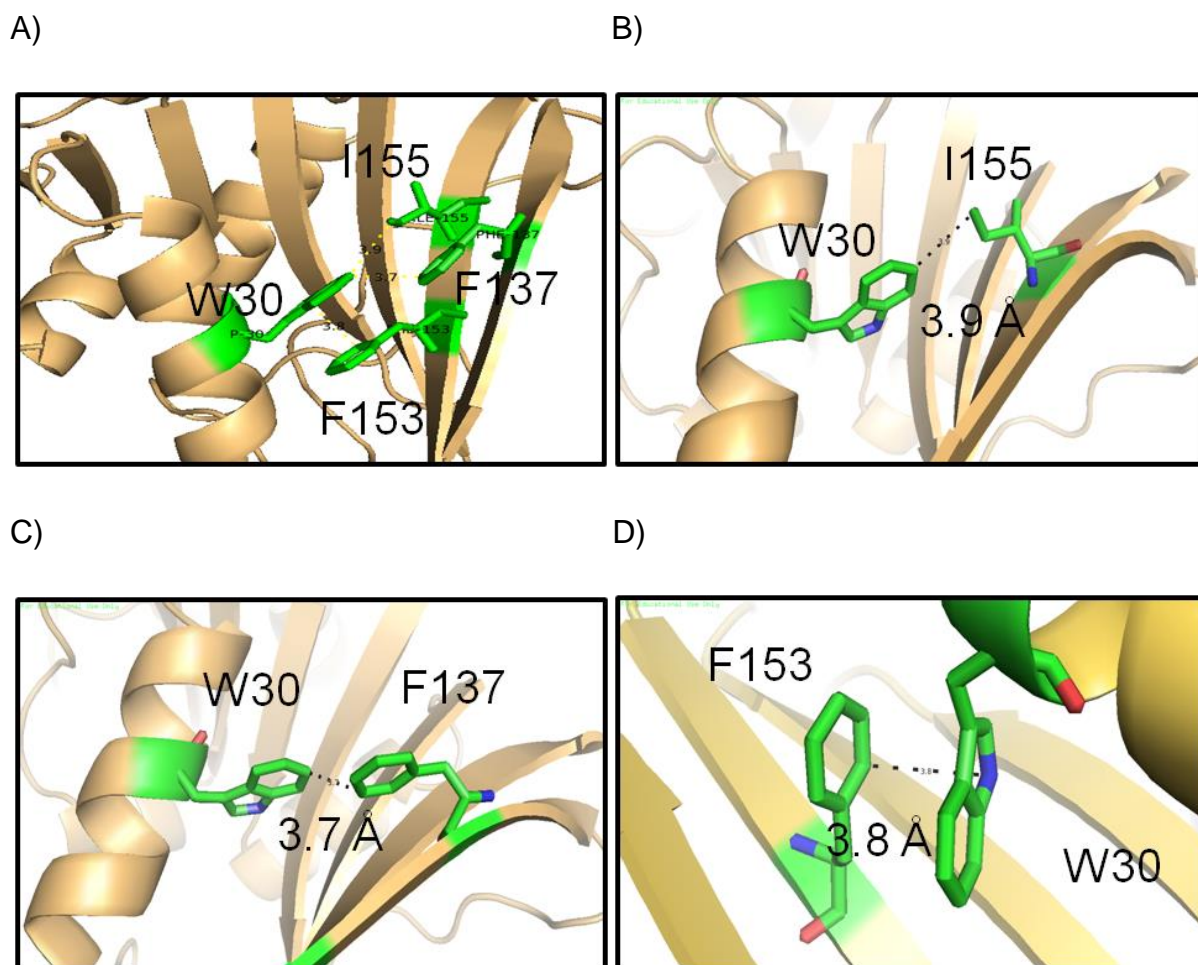


**Figure 3.3: Various interactions of residues in DHFR and their distances: A)** Interaction of W30 residue with F137, F153 and I155 residues. **B)** The distance between W30 and I155 **C)** Distance between W30 and F137 **D)** Distance between W30 and F153. All the analysis is based on crystal structure of DHFR (PDB ID: 7DFR, Resolution: 2.5Å) using PyMOL software

It was argued that if these residues do interact with W30, then mutations at any of these residues should phenocopy mutations at W30. Stability of DHFR was computationally predicted to be lowered by alanine mutations at positions F137, F153 and I155 strengthening the above hypothesis (Figure 3.4). To verify these analyses alanine mutations were made in DHFR at positions F137, F153 and I155 using site directed mutagenesis (Figure 3.5) and solubility of these mutants was characterised. As with W30 mutations, F137A, F153A and I155A also led to significant aggregation of DHFR (Figure 3.6). Thus, the destabilisation phenotype of W30 mutants may be due to loss of interaction with F137, F153 and I155.



Mutation	$\Delta\Delta G$ value	Prediction
I155A	-1.46	destabilising
F137A	-1.81	destabilising
F153A	-2.32	destabilising

**Figure 3.4: Predictions of protein stability by iMutant2.0 software:** Stability predictions of DHFR by iMutant 2.0 are shown for different mutations at positions I155, F137 and F153 where W30 was hypothesised to be interacting.

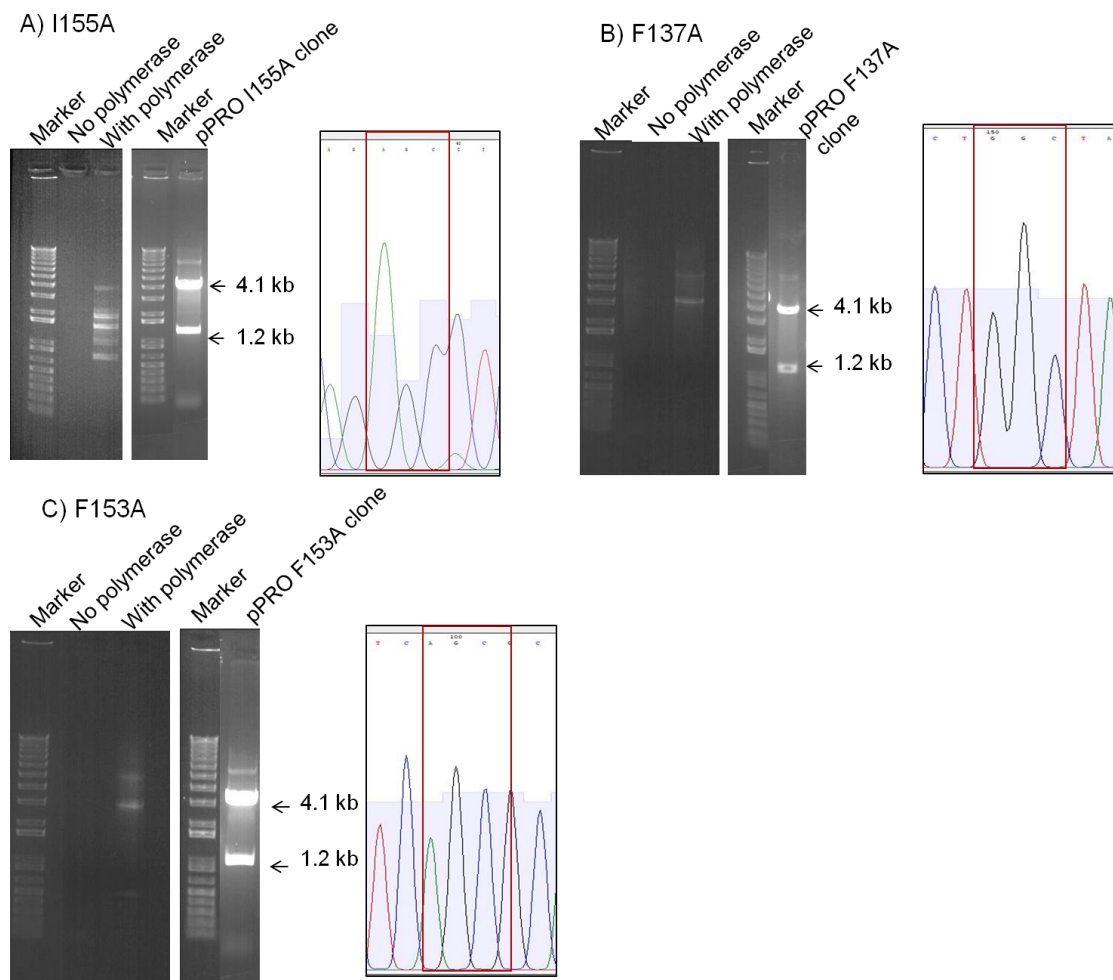


**Figure 3.5: Generation and screening of mutants on pPRO plasmid using site directed mutagenesis:** Single primer mutagenesis gel for I155A followed by *PvuI* screening and chromatogram of sequencing. A) I155A B) F137A and C) F153A

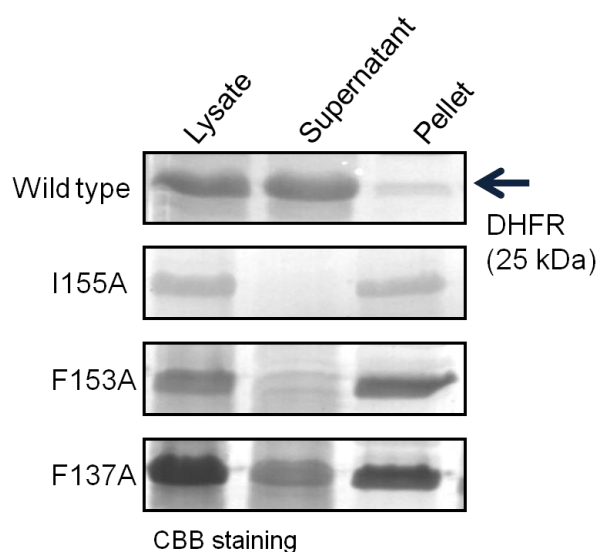
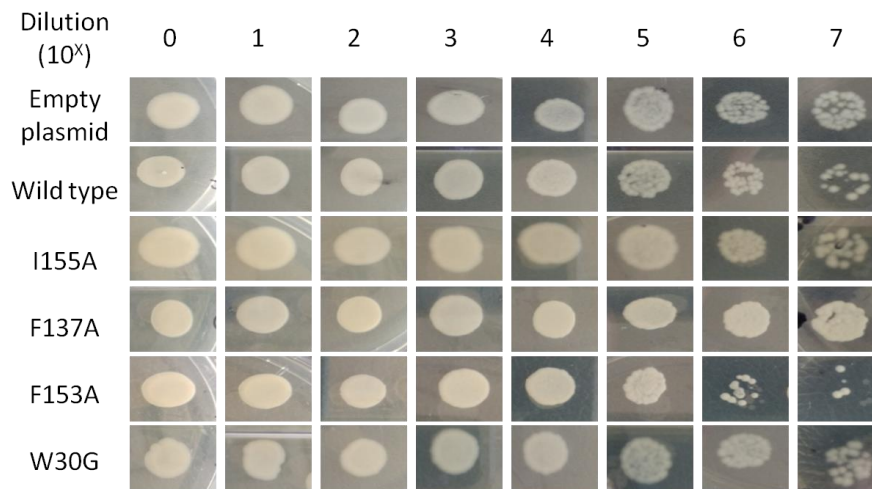


**Figure 3.6: Solubility characterisation of overexpressed wild type and mutant DHFR protein:** Lysate, supernatant and pellet fractions of wild type DHFR and different mutant DHFR on SDS page. The assay was done at 18°C.

However, it was likely that the loss in stability of F137A, F153A and I155A mutants was an independent phenotype altogether, unrelated to W30. In order to negate this possibility, the TMP-resistance levels of these strains were checked. It was argued that if the interaction between W30 and these residues was the mechanism behind the observed stability phenotypes, then the F137A, F153A and I155A mutants should also show heightened resistance, like the W30 mutants. It was found that I155A and F153A, but not F137A, were resistant to TMP (Figure 3.7 and Figure 3.8 A). Western blot analysis was also performed on each mutation to ensure that there was no significant difference in DHFR expression level between the mutants (Figure 3.8 B). This suggested that W30 may primarily interact with F153 and I155, and F137 may only contribute marginally to the observed phenotypes. Further, perturbation of these interactions could not only destabilize the DHFR protein but also confer TMP resistance.

A) TMP 0 $\mu$ g/mL



B) TMP 2 $\mu$ g/mL

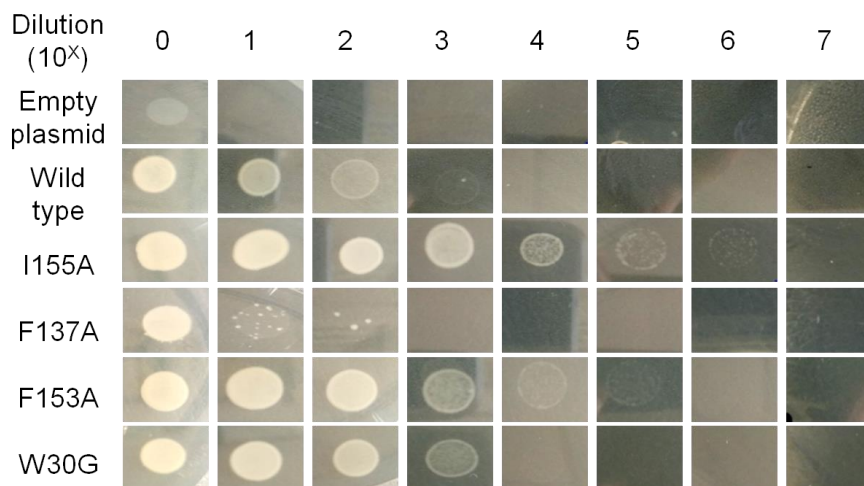
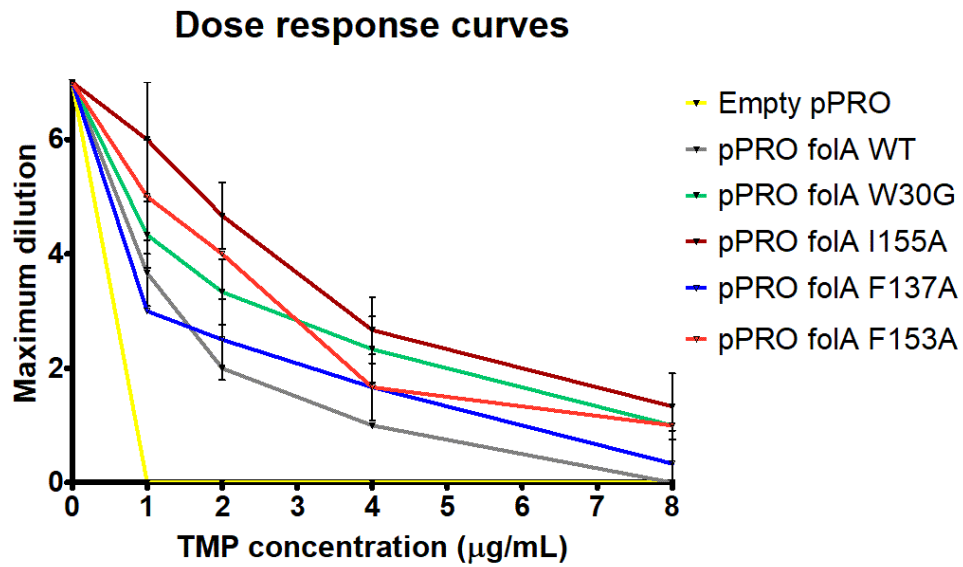


**Figure 3.7: Resistance level for different strains using dilution assay:** Strains were serially diluted spotted on LA plates supplemented with different concentrations of TMP. Images are shown here for 0  $\mu$ g /mL and 2  $\mu$ g /mL TMP for different strains.

A)



B)

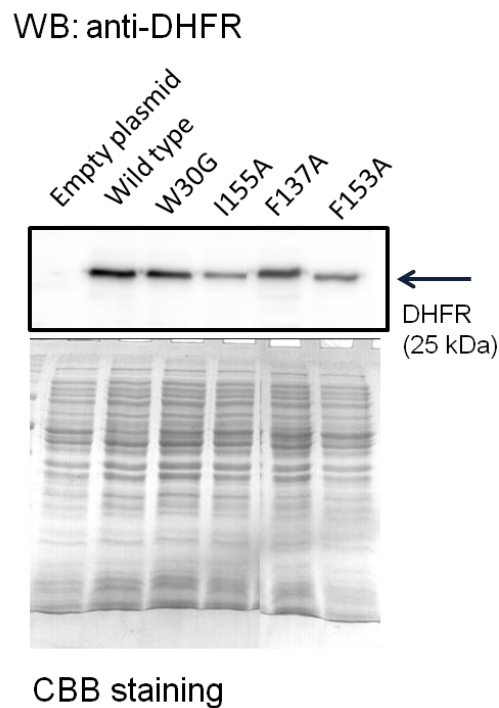


**Figure 3.8: Dose response curve for strains having different mutations in DHFR: A)** Using the spot dilution experiment, dilution number up to which growth was observed were plotted to TMP concentrations. **B)** Western blot of DHFR expression in different strains and its normalising SDS PAGE.

Tryptophan, isoleucine and phenylalanine, being hydrophobic residues, the above interactions are most likely hydrophobic interactions through residue side-chains. W30 and F153 may stack against each other as shown in Figure 3.3(D). Mutation at any of these positions would not allow these interactions to persist, leading to a perturbation of the DHFR structure and eventually instability and insolubility. Mutations at these positions also lead to trimethoprim resistance because W30 is a part of helix that forms the DHF binding site. Breaking of the interaction of W30 with F153/I155 may cause destabilisation of this helix as well which might reduce binding of TMP. Although not attempted in this project, a possible strategy to further substantiate this explanation may be to generate mutations at positions 30, 155 and 153 to re-establish interactions. For instance, mutations such as W30C and F153C can theoretically form disulfide bond between them the phenotype of the double mutant is expected to be closer to the wild type. Mutations W30R and I155Y will probably have cation- $\pi$  interaction and will probably maintain the stability of DHFR. Shown in Figure 3.9 are the possible orientations of these mutations. If these mutations rescue the solubility of DHFR and render it TMP sensitive it would further prove that the interactions of W30, I155 and W30, F137 are important for stabilisation and solubility of DHFR.

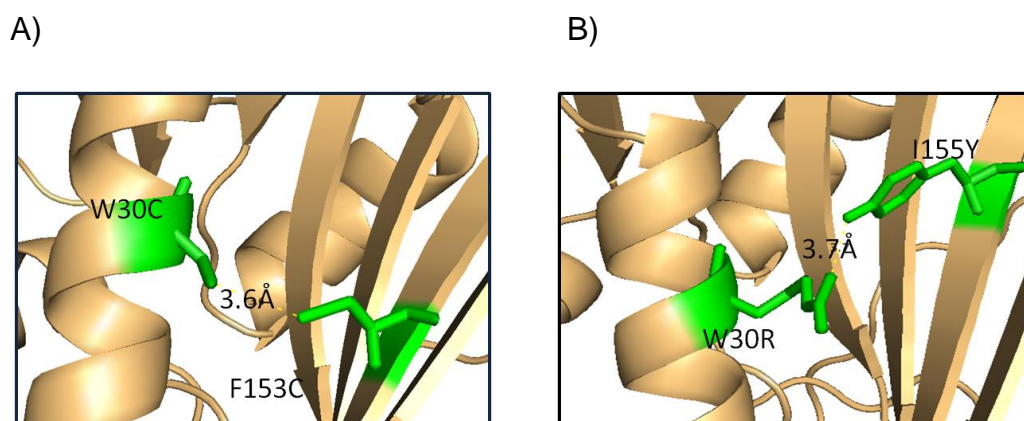


**Figure 3.9: Probable interaction of residues after mutations: A)** Probable interaction is shown for residues at 30 and 153 when mutated from W and F to cysteine respectively. **B)** Probable interaction of residues at 30 and 155 is shown for mutations from W and I to R and Y. The analysis is done in PyMOL software on the crystal structure of DHFR (PDB ID: 1RG7 and Resolution 2Å). Models of double mutants were built in SWISS-MODEL. Distances between residue side chains after mutation are indicated.

### 3.3: Effects of trimethoprim resistant mutations on the fitness of *E. coli*:

In antibiotic resistance, selection of any specific mutation and fixing in the population is dependent on the fitness of the genotype. To find out the selection dynamics of resistant bacteria it is important to assess the fitness of strains having different mutations. Therefore to check the effects of trimethoprim resistance conferring mutations on the fitness of *E. coli*, two different assays were used, namely kinetic growth curve analysis and competitive fitness. Kinetic growth curves give information about the growth of a strain individually whereas competitive fitness assay provides information about the growth of a strain relative to a competing reference strain. In these experiments, plasmid based expression of mutations will not tell the accurate effects of mutations because expression of the DHFR from the plasmid used in this study was far higher than the endogenous expression of wild type *E. coli*. Therefore TMP-resistant strains of *E. coli* harbouring mutations on the chromosomal copy of DHFR were used. These strains were obtained previously in the lab by passaging wild type *E. coli* culture in media supplemented with TMP at its IC50 (250 ng/mL) for 8 days. Resistant mutants were isolated from on TMP-supplemented plates and the *folA* locus of these strains was sequenced. From this experiment, *E. coli* strains harbouring W30G, W30C, P21Q and P21L were obtained.

Kinetic growth was analysed for the available mutants along with wild-type *E. coli* and  $\Delta folA$  strain in nutrient-rich medium (LB) and M9 defined medium (M9 supplemented with glucose (0.2%), casein hydrolysate (0.1%) and thiamine (0.5  $\mu$ g/mL). Growth kinetics was also measured in LB supplemented with thymidine to check whether thymidine could rescue the growth defects of DHFR mutants, if any. Finally, since the mutants were resistant to trimethoprim, the growth of these strains was additionally measured in the presence of trimethoprim (250 ng/mL).

The results of kinetic growth curve are shown in the Figure 3.10, 3.11, 3.12 and 3.13. The growth curves showed that performance of mutants depended on the media in which they are growing in. In LB and LB+thymidine, there was no difference seen in the growth of mutants compared to wild type. In the presence of trimethoprim, trimethoprim resistant mutants performed better compared to wild-type as expected. In M9 defined media, the performance of the W30C, W30G mutants was similar to wild type. P21Q had slightly compromised growth as compared to wild-type strain.

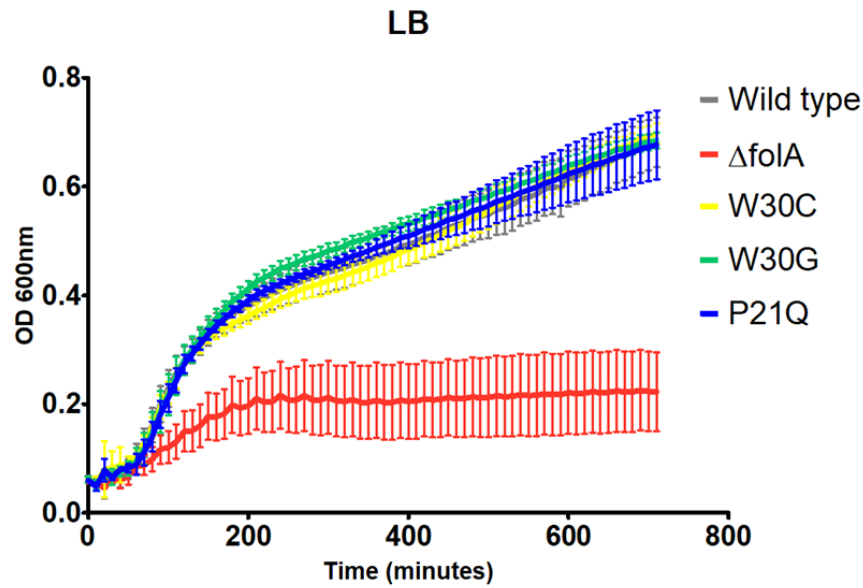


**Figure 3.10: Growth curves of different strains in LB medium:** OD600 were measured every 10 minutes for 12 hours. Data is shown as mean of four biological and 3 technical replicates with standard error.

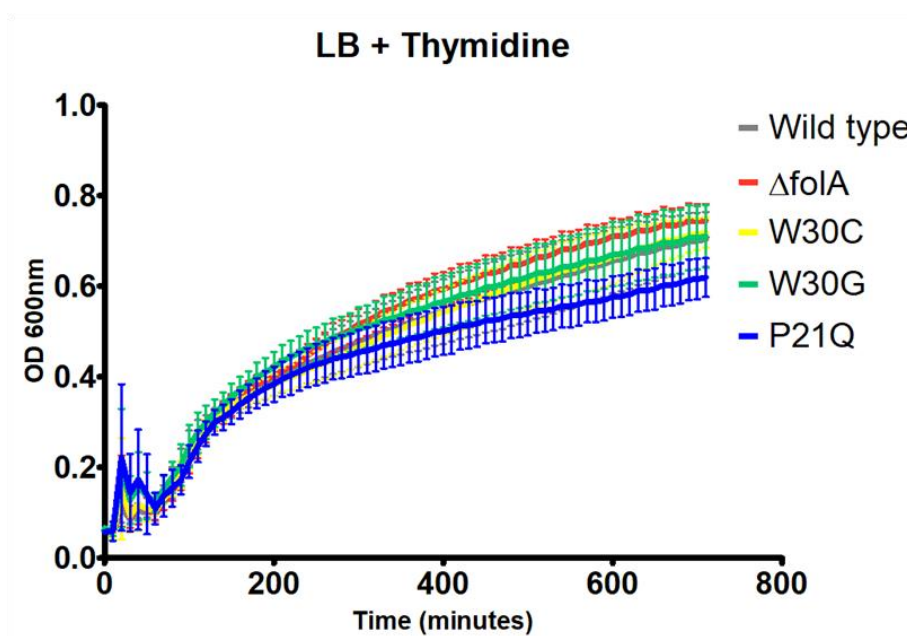


**Figure 3.11: Growth curves of different strains in LB + thymidine (100  $\mu\text{g}/\text{mL}$ ) medium:** OD600 were measured every 10 minutes for 12 hours. Data is shown as mean of four biological and 3 technical replicates with standard error.

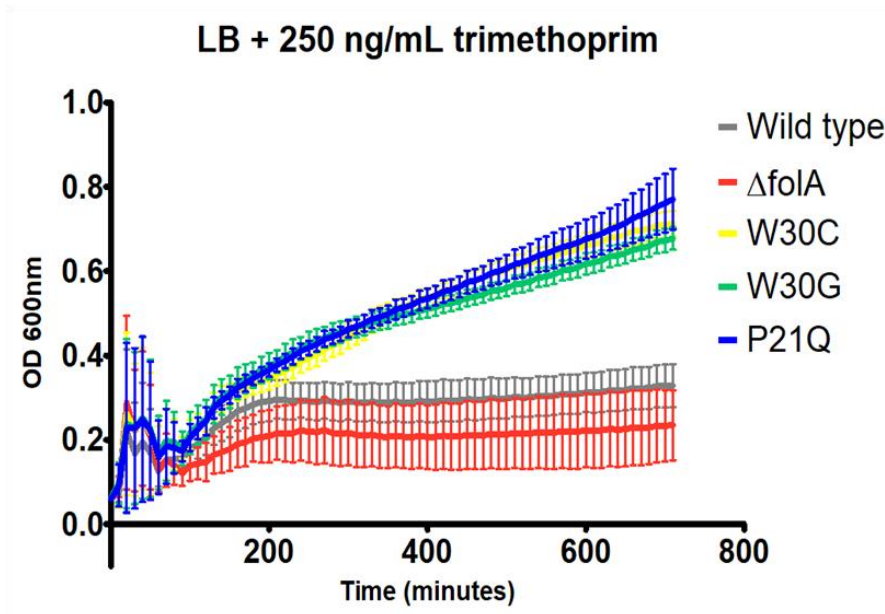


**Figure 3.12: Growth curves of different strains in LB + TMP (250 ng/mL) medium:** OD600 were measured every 10 minutes for 12 hours. Data is shown as mean of four biological and 3 technical replicates with standard error.

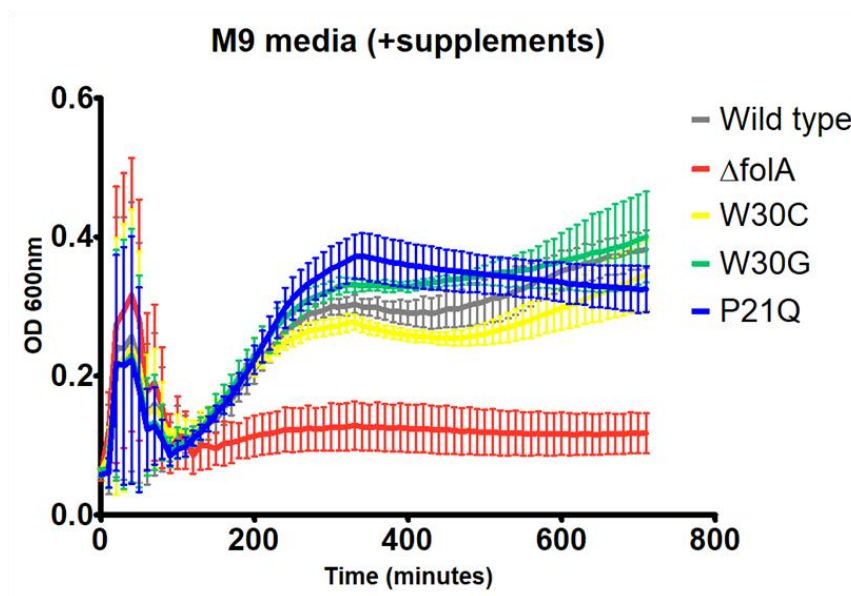


**Figure 3.13: Growth curves of different strains in M9 medium (with supplements):** OD600 were measured every 10 minutes for 12 hours. Data is shown as mean of four biological and 3 technical replicates with standard error.



To quantify the difference across strains (W30G, W30C and P21Q) two parameters were derived from the growth curves, namely carrying capacity and maximum growth rate. Optical density (OD) reached by each strain after 12 hours of growth was used as a surrogate of carrying capacity and the maximum growth rate for each strain was calculated as a change in Ln (OD) per time. The growth rates of the mutants were not significantly different from the wild type under all the tested growth conditions (Figure 3.14). It was surprising that the  $\Delta foIA$  strain, which is a thymidine auxotroph, showed some growth in LB and its growth rate was also similar to wild-type. This may be due to the presence of residual thymidine which was used for growing the primary inoculum of the strain. OD reached after 12 hours by all the trimethoprim-resistant strains was similar to wild-type in case of LB showing that in nutrient-rich medium none of the mutations had a measurable effect on growth (Figure 3.15). However, in defined media, P21Q had significantly lower maximum OD compared to wild-type whereas W30C and W30G had reached similar OD after 12 hours. In the presence of trimethoprim, growth rates of strains were unaltered but carrying capacities were higher for mutants. In a medium where LB was supplemented with thymidine, the maximum OD reached by all mutants was similar to wild type. P21Q had a slightly lower OD at 12 hours; however, this difference was not statistically significant. Overall these experiments suggested that growth of trimethoprim-mutant strains do not change in any medium except P21Q which had lower OD after 12 hours compared to wild-type. The molecular reasons behind the phenotype remain to be investigated.

### Growth rates in different conditions

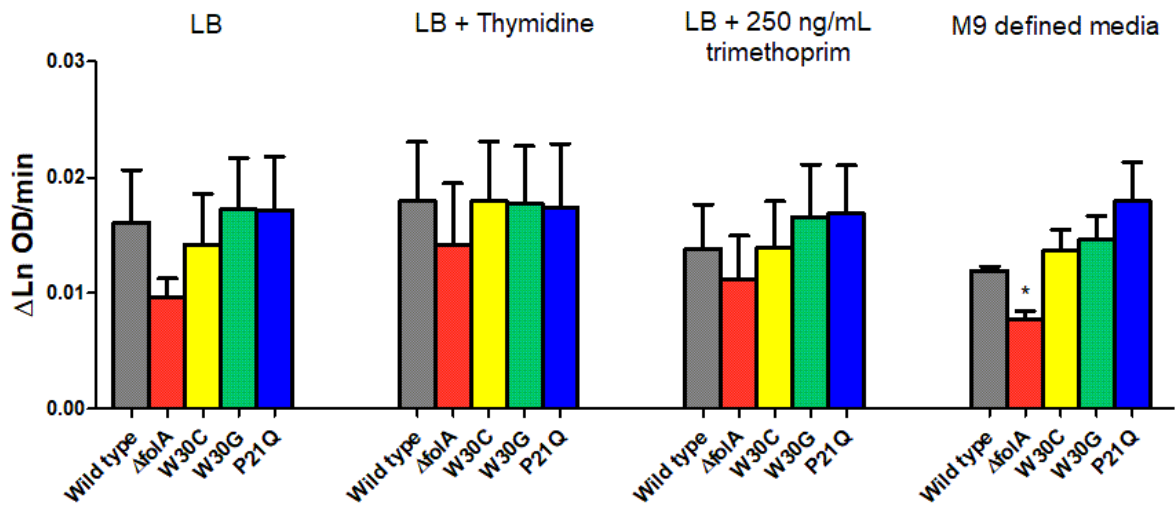


**Figure 3.14: Growth rates of TMP resistant strains in different media:** Maximum rate of change in Ln (OD) per unit time is measured and plotted as bars with standard error (4 biological replicates with 3 technical replicates). No statistically significant differences were found between growth rates.

### Comparison of OD at 12 hours

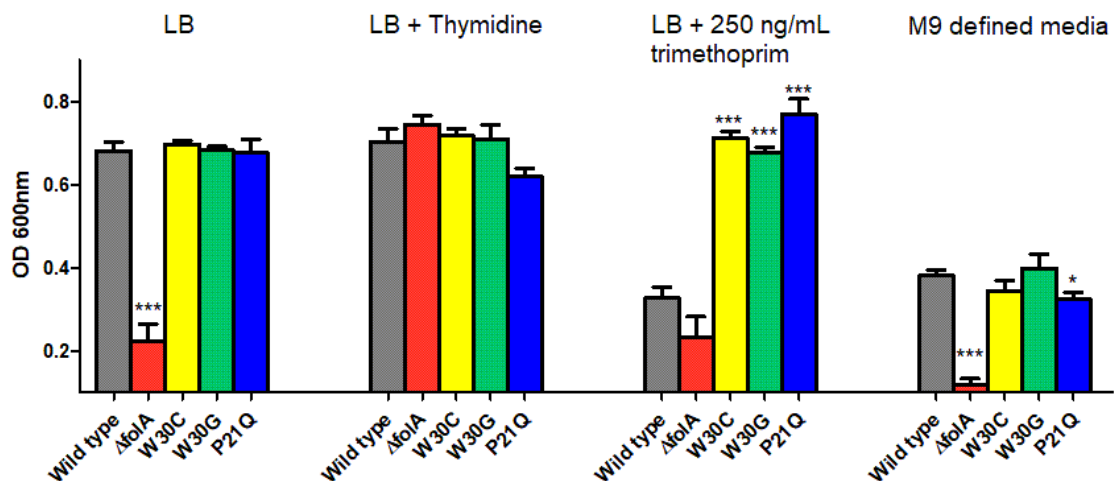


**Figure 3.15: Comparison OD after 12 hours growth of TMP resistant strains in different media:** Maximum OD reached by each strain in different condition is represented as bars with standard errors. Unpaired t-test is used for significance (4 biological replicates with 3 technical replicates) (\* $p < 0.05$ , \*\* $p < 0.01$ , \*\*\* $p < 0.001$ ).

### 3.4: Trimethoprim-resistant mutants DHFR have fitness costs:

To study effects of mutations in DHFR on the phenotype of *E. coli*, competitive fitness assays were performed and relative fitness was calculated. A  $\Delta lacZ$  variant of the wild-type strain was used as the reference strain. The fitness of wild-type strain was almost equal to 1 relative to WT  $\Delta LacZ$  strain indicating that WT  $\Delta LacZ$  strain did not have any measurable fitness cost under the growth conditions used in these experiments and hence could be used as a reference strain (Figure 3.16). Interestingly, the strain harbouring the DHFR W30G mutation was significantly less fit than the wild-type in LB medium. Strains harbouring W30C, P21Q and P21L did not show a significant fitness cost in LB. Interestingly, in defined medium, fitness cost was found in P21Q relative to wild type strain and there was not cost observed in strain W30C, W30G and P21L (Figure 3.17). The fitness cost of W30G mutant strain was nearly restored to wild-type levels in the presence of thymidine indicating that the fitness cost originated from lower active DHFR in the cell. The fitness of P21Q in defined medium was also nearly restored to wild type levels showing that somehow the absence of thymidine biosynthesis was responsible for this phenotype.

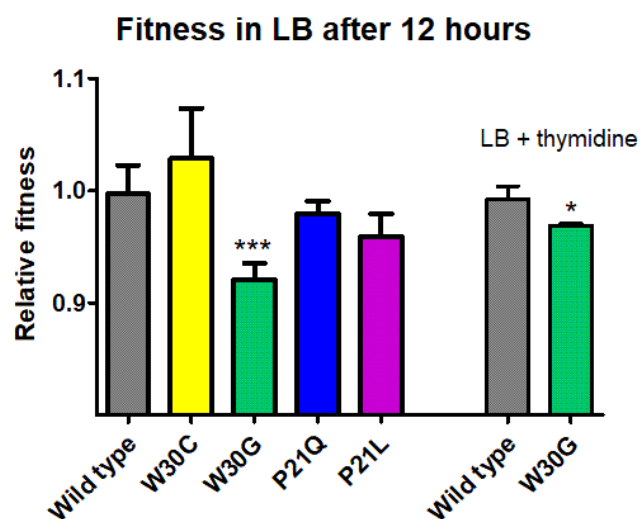


**Figure 3.16: Fitness comparisons of TMP resistant strains in LB:** Relative fitness was measured by competitive fitness assay for DHFR mutants and bars are plotted with standard deviations of values. Significance is measured by unpaired t-test (\* $p < 0.05$ , \*\* $p < 0.01$ , \*\*\* $p < 0.001$ ). At least three biological replicates were tested for LB and LB+thymidine conditions.

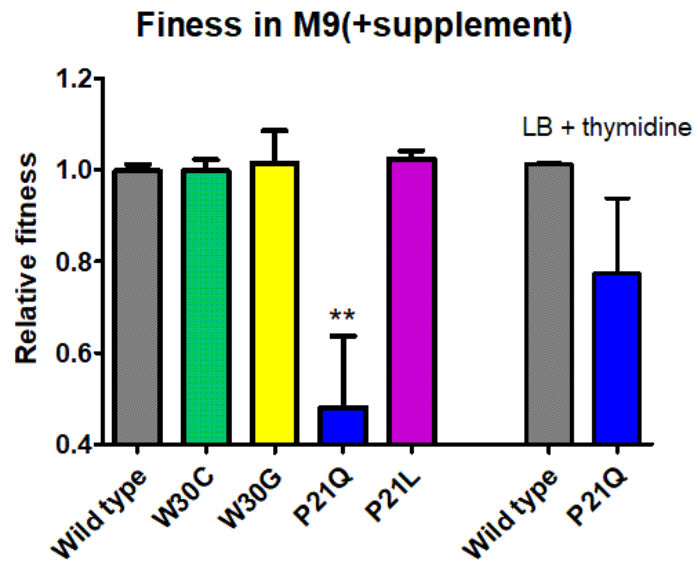


**Figure 3.17: Fitness comparisons of TMP resistant strains in LB:** Relative fitness was measured by competitive fitness assay for DHFR mutants and bars are plotted with standard deviations of values. Significance is measured by unpaired t-test (\* $p < 0.05$ , \*\* $p < 0.01$ , \*\*\* $p < 0.001$ ). At least three biological replicates tested for LB and LB+thymidine conditions.

### 3.5: Investigating the relationship between expression level of DHFR and fitness cost:

In previous studies using mutant DHFR enzymes, the expression level of DHFR and fitness was shown to be correlated (Bershtein et al., 2012). Therefore to check the correlation in the mutants which were investigated in this project, expression levels of DHFR were checked in wild type or TMP-resistant strains using Western blot analysis. It was found that regardless of the medium used the endogenous expression level of DHFR W30G was significantly lower than the wild type, W30C expression was almost equal to wild type and P21Q and P21L expression levels were higher than wild type (Figure 3.18 and 3.19). Thus, unlike earlier studies on the impact of DHFR mutations on fitness, these experiments demonstrate that expression levels of DHFR alone are not sufficient to explain the fitness of TMP-resistant mutant strains.

Fitness varies depending on medium, mutation position and the mutation. Along with expression level, fitness cost found in the strains can be dependent on the activity of available DHFR. Different in fitness can be explained by the nutrients in the medium. In case of undefined medium like LB, nutrients are in excess whereas in defined medium nutrients are limiting and this can have different effects on fitness. It was also found that different mutations fitness changes for different mutations at same site. This can be because various residues have different effect on stability of DHFR. In the case of W30G and W30C, the expression levels of W30G DHFR were consistently lower than W30C (Figure 3.18, 3.19). This can be because W30G was predicted to be more destabilising than W30C. So the W30G DHFR is probably showing the aggregation and this aggregated DHFR is getting cleared by lon protease. For W30C, the proportion of aggregated protein might be very less resulting into higher expression level than W30G and no fitness cost. The observation that W30G is costly only in LB and not in defined medium is as yet unexplained, particularly since its expression level was lower even in defined M9medium. While there is currently no explanation found for this observation, similar results have been seen in the case of other antibiotic resistant mutants. For instance, streptomycin resistant mutations of *S. enterica* where the fitness cost was found in LB source but not in the poorer carbon sources because, in poorer carbon sources there is failure of induction of RpoS ( $\sigma^s$ ) which results into translation fidelity in wild type (Paulander et al., 2009). Similarly, in case of W30G there might be change in cellular physiology in LB and defined medium that can alter the fitness.

P21L and P21Q both had higher expression levels compared to wild type DHFR. P21 residue is found in M20 catalytic loop in DHFR. Mutations at P21 probably reduce the expression levels initially and negative feedback loop might be increasing the expression for compensation of activity. Using iMutant stability predictions, the P21L mutation was not destabilising ( $\Delta\Delta G = 0.46$ ) whereas P21Q was slightly destabilising ( $\Delta\Delta G = -0.52$ ) (Figure 3.2 B). The solubility characterisation also showed that P21Q strain had lower solubility than P21L as an equal part of P21Q was found to be in pellet and supernatant fraction when overexpressed (Figure 3.1). This difference suggests that in M9 medium where there are fixed nutrients P21Q DHFR may not be able to catalysed the reaction compared to wild type strain. In LB medium, there are excess nutrient present which may compensate the function of

P21Q DHFR and help the strain grow equally like wild type strain. As the phenotype of P21Q was rescued by thymidine, fitness of P21Q might be dependent on catalytic activity.

Overall the experimental results outlined in this project suggest that trimethoprim resistant mutations have different effects on the structure of DHFR which may translate into fitness costs (Figure 3.1, 3.2B, 3.16, 3.17). The fitness of TMP-resistant strains were only partially explained by expression level of DHFR contrary to earlier reports (Bershtein et al., 2012). Indeed, the fitness of TMP-resistant strains was determined by many factors including mutation position, mutation type and nutrients in the medium (Figure 3.16, 3.17). All of these together may contribute the selection of TMP resistant bacteria. More genetic, structural and biochemical analyses are required to find the changes in other pathways which modulate the fitness effects of TMP-resistant bacteria.

WB: anti-DHFR

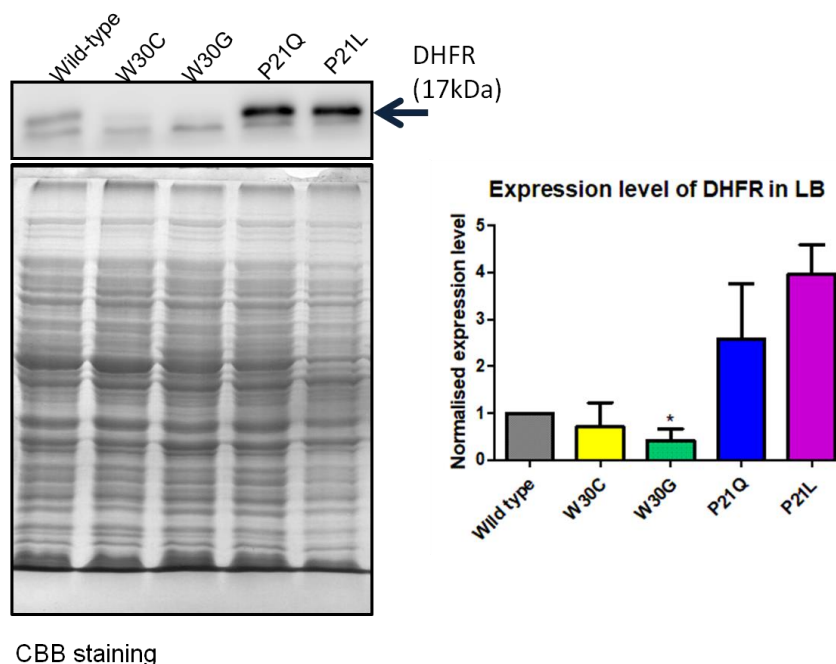


**Figure 3.18: Western blot for natural expression of chromosomally encoded DHFR and its different mutants in LB medium:** Level of DHFR was determined by immunoblotting. The SDS PAGE of lysates of indicated strains is shown as the normalising gel. Quantification of blot was done in ImageJ and expression levels normalized to wild type were plotted. Mean with standard deviations are shown (paired t test, \*p <0.05, \*\*p <0.01, \*\*\*p <0.001).

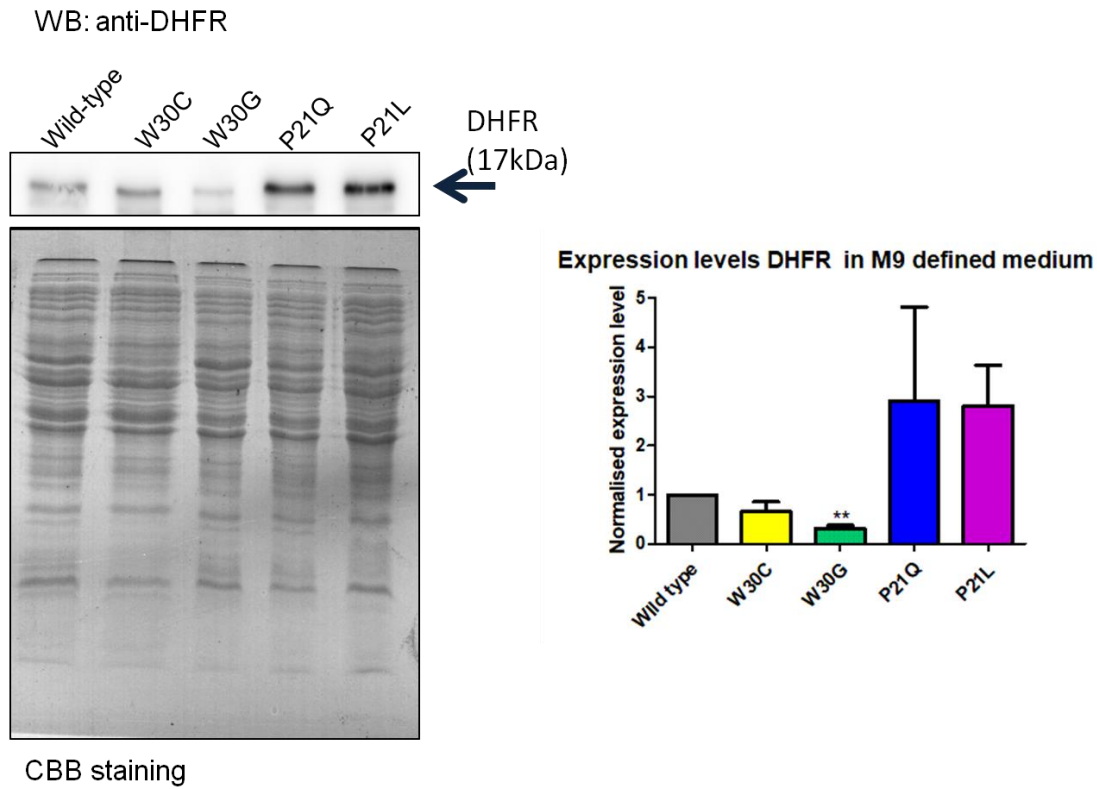


**Figure 3.19: Western blot for natural expression of chromosomally encoded DHFR and its different mutants in M9 defined medium:** Level of DHFR was determined by immunoblotting. The SDS PAGE of lysates of indicated strains is shown as the normalising gel. Quantification of blot was done in ImageJ and expression levels normalized to wild type were plotted. Mean with standard deviations are shown (paired t test, \* $p < 0.05$ , \*\* $p < 0.01$ , \*\*\* $p < 0.001$ ).

## **CHAPTER 4:**

### **SUMMARY AND FUTURE DIRECTIONS**

#### **Summary:**

In this project, the impact of trimethoprim resistance conferring mutations on aggregation of DHFR, trimethoprim resistance and fitness was analysed in *E. coli*. There was also an attempt to investigate the molecular mechanisms behind these effects. In the first part of this study, it was shown that mutation of W30G, W30R and W30C in *E. coli* DHFR promotes aggregation and reduces the solubility of this enzyme in addition to conferring TMP-resistance (Section 3.1). Using structural and mutational analyses I155, F153 and F137 residues of DHFR were shown to interact with W30 and these interactions were demonstrated to be important for the solubility of DHFR (Figure 3.3). Additionally, Ala substitutions at I155 and F153, but not F137, were also found to confer TMP resistance suggesting that interactions between W30, F153 and W30, I155 may be of primary importance (Figure 3.7, 3.8).

In the second part of this project, the consequences of stability effects of mutations on the expression levels of DHFR were investigated. It was found that W30G mutation reduced the expression level of DHFR (Figure 3.18, 3.19). This impact on stability and expression level was also resulted in a reduction of fitness for W30G mutants (Figure 3.16). Interestingly, there was an increase in expression levels of DHFR in the case of P21L and P21Q mutations and unexpectedly the P21Q mutation also had a fitness cost. The fitness costs of W30G and P21Q were growth condition-specific and both could be rescued by thymidine addition in the growth medium, suggesting that the cost is due to aggregation toxicity but lower DHFR activity (Figure 3.16, 3.17). Fitness costs were not found for other mutants like W30C and P21L under the growth conditions tested in this study (Figure 3.16, 3.17) indicating that not all TMP-resistant mutations in DHFR are costly.

These studies demonstrate that TMP resistant mutations can have effects on the structure of DHFR and also on the fitness of *E. coli*. Expression levels of DHFR play a role in deciding fitness of strain along with other factors which are yet to be determined.



## Future directions:

In the project, it was found that mutations at W30 (W30G, W30C and W30R) resulted in the mis-folding of DHFR. Structural analysis showed the possibility of interaction of W30, I155 and W30 and F153. It was already shown that Ala mutations at I155 and F1153 can show same phenotype (Insolubility of DHFR and TMP resistance) as W30 mutants and hence is a possible mechanism for the observed effects of W30 mutations. To further validate this hypothesis, one would require to engineer mutations at I155 and F153 that can rescue the phenotypes of W30 mutations by reestablishing interactions. The proposed plan is to make the W30R-I155Y and W30C-F153C double mutants, in which interactions are expected to be reestablished.

To check the effects of TMP resistant mutations on fitness, mutated strains (W30G, W30C, P21Q and P21L) were obtained by exposure of IC50 TMP to wild type *E. coli* subsequently by sequencing *folA* locus. The strains obtained from this process may harbour mutations in chromosome other than at *folA* locus. To specifically get the results there is a need for engineering DHFR mutations (W30G, W30C, P21Q and P21L) *E. coli* chromosome and confirm the results of this study. This may be done using genome engineering protocols that have been used in the past for DHFR (Datsenko and Wanner, 2000).

In this study, it was also found that expression level of W30G DHFR was low compared to wild type DHFR and that this possibly explained the fitness cost associated with W30G mutation. The expression level of W30G may have been low due to its aggregation. It has been previously demonstrated that aggregated DHFR is proteolysed by Lon protease (Rodrigues et al., 2016). Thus, a deletion in the Lon protease may rescue the phenotype of the W30G mutant. The second possibility can be overexpression of GroEL/ES chaperons (which helps the misfolded protein to fold properly) in DHFR mutant strain (W30G, W30R and W30C) to check the role of aggregation in the fitness cost.

To find the mechanism of fitness variation in different growth conditions, fitness analysis can be done for DHFR mutants in various growth conditions like in changing carbon source or inclusion of molecules in media which are in the folate biosynthetic

pathways which will provide insight about the factors which are involved in the fitness of TMP resistant mutants.

# APPENDIX

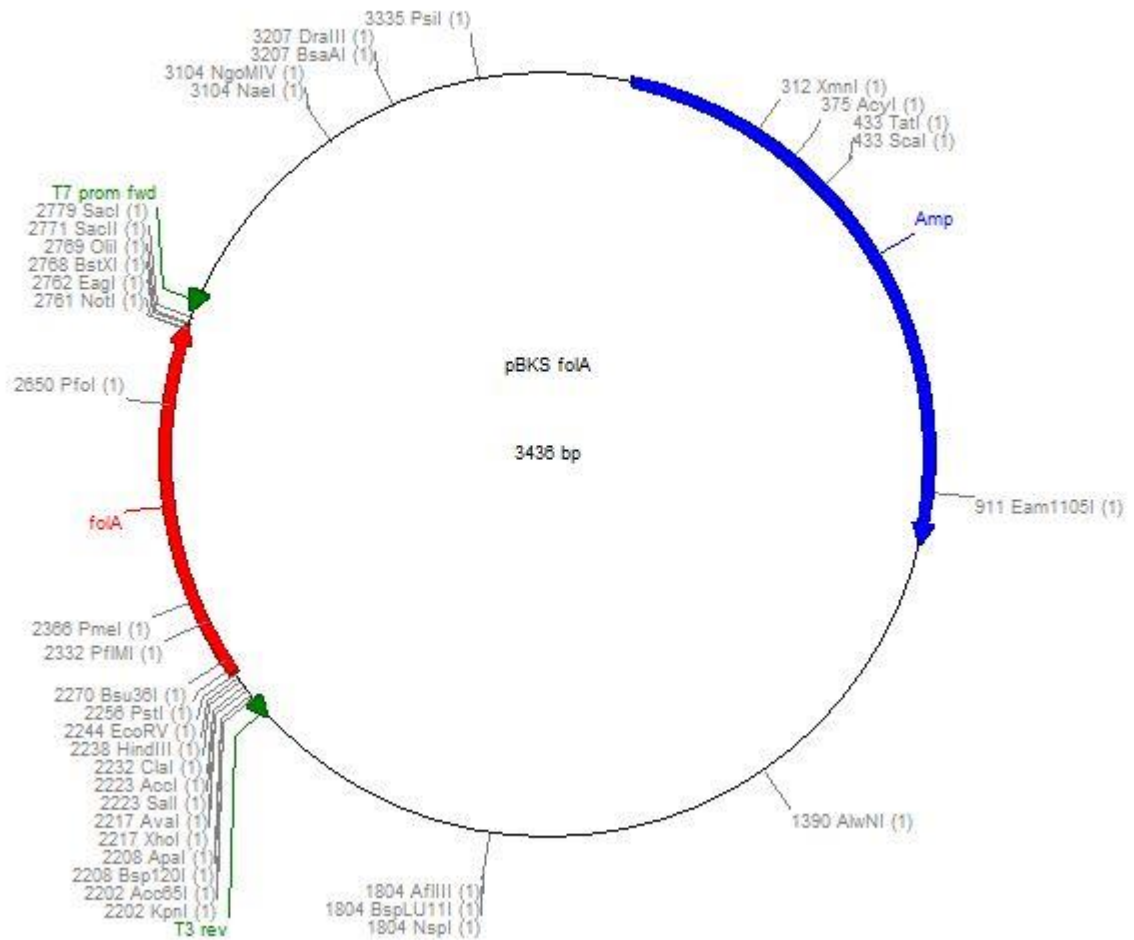


Figure 5.1: Vector map of BKS plasmid which was used as template for generation of mutants

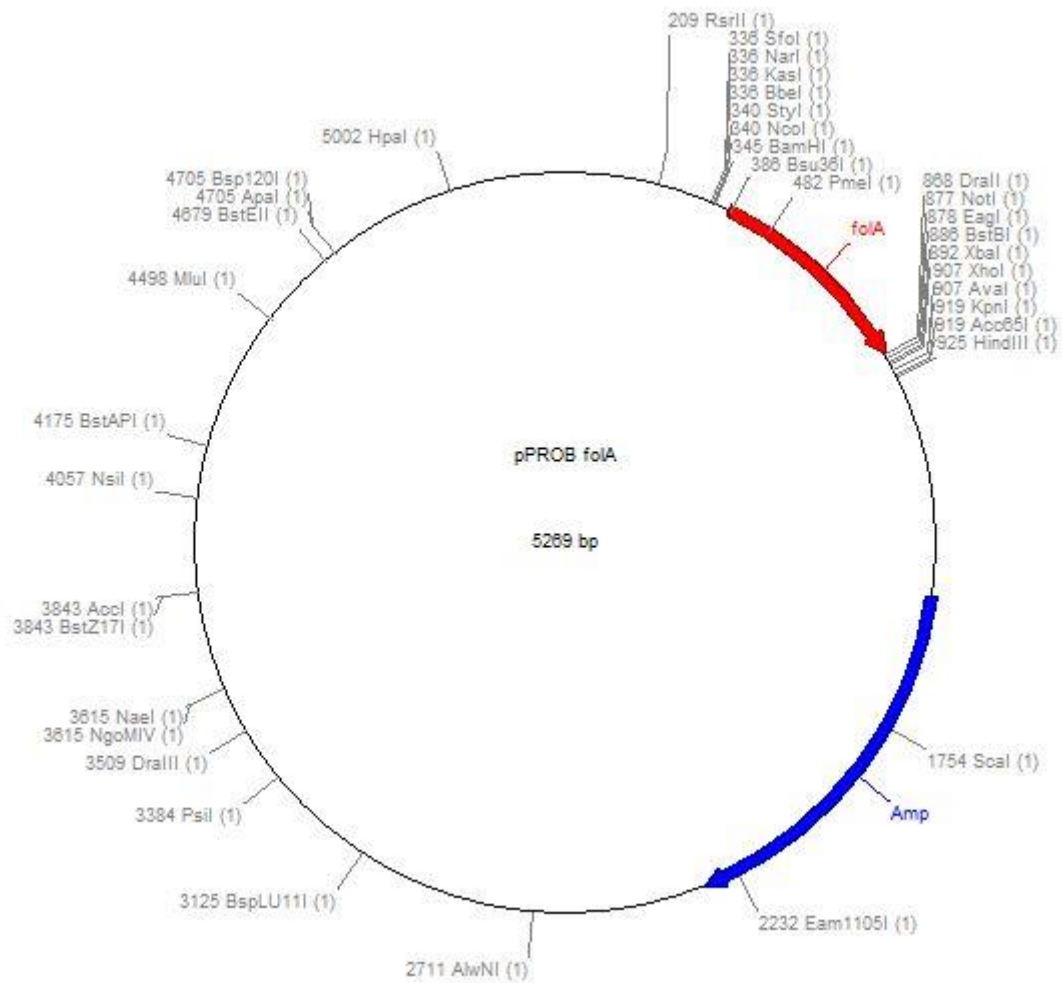


Figure 5.2: Vector map of pPRO plasmid which was used as template for generation of mutants

# **BIBLIOGRAPHY**

1. Adersson, D.I., and Hughes, D. (2010). Antibiotic resistance and its cost: is it possible to reverse resistance? *Nat. Rev. Microbiol.* 8, 260–271.
2. Andersson, D.I., and Hughes, D. (2014). Microbiological effects of sublethal levels of antibiotics. *Nat. Rev. Microbiol.* 12, 465–478.
3. Baughman, G.A., and Fahnestock, S.R. (1979). Chloramphenicol resistance mutation in *Escherichia coli* which maps in the major ribosomal protein gene. *Chloramphenicol Resistance Mutation in Escherichia coli Which Maps in the Major Ribosomal Protein Gene Cluster.* 137, 1315–1323.
4. Bershtein, S., Mu, W., and Shakhnovich, E.I. (2012). Soluble oligomerization provides a beneficial fitness effect on destabilizing mutations. *Proc. Natl. Acad. Sci.* 109, 4857–4862.
5. Bhabha, G., Ekiert, D.C., Jennewein, M., Zmasek, C.M., Tuttle, L.M., Kroon, G., Dyson, H.J., Godzik, A., Wilson, I.A., and Wright, P.E. (2013). Divergent evolution of protein conformational dynamics in dihydrofolate reductase. *Nat. Struct. Mol. Biol.* 20, 1243–1249.
6. Boehr, D.D., McElheny, D., Dyson, H.J., and Wright, P.E. (2006). The Dynamic Energy Landscape of Dihydrofolate Reductase Catalysis. *Science* (80- ). 313, 1638–1642.
7. Böttger, E.C., and Springer, B. (2008). Tuberculosis: Drug resistance, fitness, and strategies for global control. *Eur. J. Pediatr.* 167, 141–148.
8. Bradford, M.M. (1976). A rapid and sensitive method for the quantitation of microgram quantities of protein utilizing the principle of protein-dye binding. *Anal. Biochem.* 72, 248–254.
9. Bradford, P.A. (2001). Extended-spectrum beta-lactamases in the 21st century: characterization, epidemiology, and detection of this important resistance threat. *Clin. Microbiol. Rev.* 14, 933–51, table of contents.
10. Brolund, A., Sundqvist, M., Kahlmeter, G., and Grape, M. (2010). Molecular characterisation of trimethoprim resistance in *Escherichia coli* and *Klebsiella pneumoniae* during a two year intervention on trimethoprim use. *PLoS One* 5, 1–5.

11. Bystroff, C., Oatley, S.J., and Kraut, J. (1990). Crystal structures of Escherichia coli dihydrofolate reductase: the NADP<sup>+</sup> holoenzyme and the folate .cntdot. NADP<sup>+</sup> ternary complex. substrate binding and a model for the transition state. *Biochemistry* 29, 3263–3277.
12. Capriotti, E., Fariselli, P., and Casadio, R. (2005). I-Mutant2.0: Predicting stability changes upon mutation from the protein sequence or structure. *Nucleic Acids Res.* 33, 306–310.
13. Chumpia, W., Ohsato, T., Kuma, H., Ikeda, S., Hamasaki, N., and Kang, D. (2003). Affinity purification of antibodies by using Ni 2 p -resins on which inclusion body-forming proteins are immobilized. 32, 147–150.
14. Datsenko, K., and Wanner, B.L. (2000). One-step inactivation of chromosomal genes in Escherichia coli K-12 using PCR products. *Proc Natl Acad Sci USA* 97, 6640–6645.
15. Flensburg, J., and Sköld, O. (1987). Massive overproduction of dihydrofolate reductase in bacteria as a response to the use of trimethoprim. *Eur. J. Biochem.* 162, 473–476.
16. Ghafourian, S., Sadeghifard, N., Soheili, S., and Sekawi, Z. (2014). Extended spectrum beta-lactamases: Definition, classification and epidemiology. *Curr. Issues Mol. Biol.* 17, 11–22.
17. Jacquier, H., Birgy, A., Le Nagard, H., Mechulam, Y., Schmitt, E., Glodt, J., Bercot, B., Petit, E., Poulain, J., Barnaud, G., et al. (2013). Capturing the mutational landscape of the beta-lactamase TEM-1. *Proc. Natl. Acad. Sci.* 110, 13067–13072.
18. Klesmith, J.R., Bacik, J.-P., Wrenbeck, E.E., Michalczyk, R., and Whitehead, T.A. (2017). Trade-offs between enzyme fitness and solubility illuminated by deep mutational scanning. *Proc. Natl. Acad. Sci.* 114, 2265–2270.
19. Laxminarayan, R., Duse, A., Wattal, C., Zaidi, A.K.M., Wertheim, H.F.L., Sumpradit, N., Vlieghe, E., Hara, G.L., Durand, C.G., and Aires, B. (2013). Antibiotic resistance — the need for global solutions. 13.
20. Maskell, J.P., Sefton, A.M., and Hall, L.M.C. (2001). Multiple mutations modulate the function of dihydrofolate reductase in trimethoprim-resistant *Streptococcus pneumoniae*. *Antimicrob. Agents Chemother.* 45, 1104–1108.
21. Nikaido, H. (1998). Antibiotic Resistance Caused by Gram-Negative Multidrug Efflux Pumps. 27, 32–41.

22. Otto, M. (2013). NIH Public Access. *14*, 1513–1521.
23. Palmer, A.C., and Kishony, R. (2014). Opposing effects of target overexpression reveal drug mechanisms. *Nat. Commun.* *5*, 4296.
24. Palmer, A.C., Toprak, E., Baym, M., Kim, S., Veres, A., Bershtein, S., and Kishony, R. (2015). Delayed commitment to evolutionary fate in antibiotic resistance fitness landscapes. *Nat. Commun.* *6*, 7385.
25. Paulander, W., Maisnier-Patin, S., and Andersson, D.I. (2009). The fitness cost of streptomycin resistance depends on rpsL mutation, carbon source and RpoS ( $\sigma$ S). *Genetics* *183*, 539–546.
26. Ramirez, M.S., Traglia, G.M., Lin, D.L., Tran, T., and Tolmasky, M.E. (2014). Plasmid-Mediated Antibiotic Resistance and Virulence in Gramfile:///C:/Users/hp-pc/Desktop/tolerance.nbib-negatives: the *Klebsiella pneumoniae* Paradigm. *Microbiol. Spectr.* *2*, 1–15.
27. Riley, M., Abe, T., Arnaud, M.B., Berlyn, M.K.B., Blattner, F.R., Chaudhuri, R.R., Glasner, J.D., Horiuchi, T., Keseler, I.M., Kosuge, T., et al. (2006). *Escherichia coli* K-12: a cooperatively developed annotation snapshot--2005. *Nucleic Acids Res.* *34*, 1–9.
28. Rodrigues, J. V., Bershtein, S., Li, A., Lozovsky, E.R., Hartl, D.L., and Shakhnovich, E.I. (2016). Biophysical principles predict fitness landscapes of drug resistance. *Proc. Natl. Acad. Sci.* *113*, E1470–E1478.
29. Saunders, J.R., Hart, C.A., and Saunders, V.A. (1986). Plasmid-mediated resistance to beta-lactam antibiotics in gram-negative bacteria: the role of in-vivo recyclization reactions in plasmid evolution. *J. Antimicrob. Chemother.* *18 Suppl C*, 57–66.
30. Schnell, J.R., Dyson, H.J., and Wright, P.E. (2004). Structure, Dynamics, and Catalytic Function of Dihydrofolate Reductase. *Annu. Rev. Biophys. Biomol. Struct.* *33*, 119–140.
31. Shaw, K.J., Rather, P.N., Hare, R.S., and Miller, G.H. (1993). Molecular genetics of aminoglycoside resistance genes and familial relationships of the aminoglycoside-modifying enzymes. *Microbiol. Rev.* *57*, 138–163.
32. Shenoy, A.R., and Visweswariah, S.S. (2003). Site-directed mutagenesis using a single mutagenic oligonucleotide and Dpn I digestion of template DNA. *319*, 335–336.

33. Studer, R.A., Dessailly, B.H., and Orengo, C.A. (2013). Residue mutations and their impact on protein structure and function : detecting beneficial and pathogenic changes. *594*, 581–594.
34. Subirats, J., Sànchez-melsió, A., Borrego, C.M., Balcázar, J.L., and Simonet, P. (2016). Metagenomic analysis reveals that bacteriophages are reservoirs of antibiotic resistance genes. *Int. J. Antimicrob. Agents* 1–5.
35. Sun, J., Deng, Z., and Yan, A. (2014). Bacterial multidrug efflux pumps: Mechanisms, physiology and pharmacological exploitations. *Biochem. Biophys. Res. Commun.* *453*, 254–267.
36. Vogwill, T., and Maclean, R.C. (2015). The genetic basis of the fitness costs of antimicrobial resistance: A meta-analysis approach. *Evol. Appl.* *8*, 284–295.
37. Waksman, S. a (2011). Mycological Society of America WHAT IS AN ANTIBIOTIC OR AN ANTI- BIOTIC SUBSTANCE ? \*. America (NY). *39*, 565–569.
38. Watson, M., Liu, J.-W., and Ollis, D. (2007). Directed evolution of trimethoprim resistance in *Escherichia coli*. *FEBS J.* *274*, 2661–2671.
39. Wiser, M.J., and Lenski, R.E. (2015). A comparison of methods to measure fitness in *Escherichia coli*. *PLoS One* 1–11.
40. Zarantonelli, L., Borthagaray, G., Lee, E.H., Veal, W., and Shafer, W.M. (2001). Decreased susceptibility to azithromycin and erythromycin mediated by a novel mtr(R) promoter mutation in *Neisseria gonorrhoeae*. *J. Antimicrob. Chemother.* *47*, 651–654.